Applying the effective-source approach to frequency-domain self-force calculations: Lorenz-gauge gravitational perturbations

Barry Wardell[1,2] and Niels Warburton[3,2]

[1]*Department of Astronomy, Cornell University, Ithaca, New York 14853, USA*
[2]*School of Mathematical Sciences and Complex & Adaptive Systems Laboratory,*
University College Dublin, Belfield, Dublin 4, Ireland
[3]*MIT Kavli Institute for Astrophysics and Space Research, Massachusetts Institute of Technology,*
Cambridge, Massachusetts 02139, USA

With a view to developing a formalism that will be applicable at second perturbative order, we devise a new practical scheme for computing the gravitational self-force experienced by a point mass moving in a curved background spacetime. Our method works in the frequency domain and employs the effective-source approach, in which a distributional source for the retarded metric perturbation is replaced with an effective source for a certain regularized self-field. A key ingredient of the calculation is the analytic determination of an appropriate puncture field from which the effective source and regularized residual field can be calculated. In addition to its application in our effective-source method, we also show how this puncture field can be used to derive tensor-harmonic mode-sum regularization parameters that improve the efficiency of the traditional mode-sum procedure. To demonstrate the method, we calculate the first-order-in-the-mass-ratio self-force and redshift invariant for a point mass on a circular orbit in Schwarzschild spacetime.

I. INTRODUCTION

The detection of gravitational waves from inspiraling compact binary systems will be greatly assisted by theoretical waveform templates. Using matched filtering techniques, these templates will help to extract the incoming signal from the detector noise and, once detection becomes routine, the same templates will allow the parameters of the source binary systems to be established. Constructing an appropriate bank of waveform templates necessitates understanding the two-body problem in the general-relativistic context. Unlike its Newtonian counterpart, this problem cannot be solved analytically with closed-form solutions. Instead, a variety of methods exist to approximate the solution, each best suited to a particular set of system parameters.

To model binary systems of comparable mass and small orbital separation it is necessary to turn to numerical simulations to solve the full nonlinear Einstein field equations. Numerical relativity has made great progress in recent years and it is now routine to numerically evolve binary systems of comparable-mass black holes or neutron stars through tens of orbits up to, and through, merger [1,2]. Aside from numerical truncation error, these results are exact. However, the computational cost of running simulations to merger increases rapidly as the mass ratio of the smaller to the more massive body is decreased. The computational cost similarly increases as the initial orbital separation increases. Consequently, in these domains other approaches are required.

For systems with large orbital separation the post-Newtonian (PN) expansion can be employed. This is a perturbative approach to the problem that involves expanding the field equations in powers of the orbital velocity as a fraction of the speed of light. This approach has a long and rich history and today the post-Newtonian expansion of the dynamics of a binary is now known up to 3PN order, with many 4PN terms now known; see Ref. [3] for a recent review.

When one of the bodies is substantially more massive than the other the small mass ratio of the system can be used as a perturbative parameter. In this approach the less massive of the two bodies is usually modeled as a point particle. Flux balance arguments allow the dissipative dynamics to be modeled [4,5], but in order to include conservative corrections it is necessary to evaluate the local "self-force" acting on the particle. With a point-particle source this then necessitates a regularization procedure to remove the Coulomb-like divergence of the metric perturbation that does not contribute to the orbital dynamics. Over the years this regularization procedure has been placed on very firm theoretical footing at first order in the mass ratio [6–8] and recently has been understood at second perturbative order [9–11].

At first perturbative order a large number of practical self-force calculations have been made; see Ref. [12] for a recent review. Practical calculation techniques are often prototyped with scalar-field toy models before the gravitational case is considered. In both cases motion in the spherically symmetric Schwarzschild spacetime is usually tackled first, before turning attention to motion in the more astrophysically relevant Kerr spacetime of a rotating black hole.

In recent years, the calculation of gauge-invariant quantities has proven to be particularly fruitful as it allows for comparison of self-force results with those of post-Newtonian

theory and numerical relativity. A number of these gauge-invariant quantities are now known [13–16] and using them to make cross-cultural comparisons has been illuminating; they help to delineate the region in which perturbative approaches are valid, as well as act as a cross-check on the widely different computational approaches taken by each scheme. One particularly interesting result is that of Le Tiec *et al.* [17] which showed that even for comparable-mass systems perturbative methods can make meaningful statements about the orbital dynamics. Calibrating effective-one-body theory is another important use for gauge-invariant results [18–20].

When making self-force calculations, an important consideration is the practical regularization technique to be employed. All the techniques derive from the same fundamental regularization procedure, but different techniques suit different calculational approaches. One of the most commonly employed techniques is the mode-sum prescription [21]. This approach relies on the mode decomposition rendering the individual modes of the retarded-field solution finite at the particle's location and has had much success with $1 + 1$ time-domain and frequency-domain calculations. For $2 + 1$ or $3 + 1$ time-domain decompositions, where the retarded field remains divergent at the particle, so-called "effective source" techniques were developed [22,23]. This approach involves moving the contribution from the singular metric perturbation near the particle into the source. This procedure renders the otherwise divergent source finite and amenable to numerical treatment.

To date all self-force calculations have been at first order in the mass ratio. The key motivation for the present work is to develop a set of techniques that can extend the work mentioned above to encompass second-order-in-the-mass-ratio calculations, with the aim of computing conservative gauge-invariant quantities [24]. This immediately suggests the basic form our approach should take.

(1) Work in the Lorenz gauge. Currently the regularization procedure at second order in the mass ratio is best understood in the Lorenz gauge [9,25].

(2) Work in the frequency domain. At present it is not known how to stably evolve the monopole and dipole contributions to the Lorenz-gauge linearized Einstein equation [26]. These instabilities are observed in $1 + 1$-, $2 + 1$-, and $3 + 1$-dimensional time-domain decompositions on a Schwarzschild background, and similar instabilities have been seen in Kerr spacetime [27]. Even if the multipole $l \geq 2$ modes are evolved separately in the time domain, the $\ell = 0, 1$ modes must be solved in the frequency domain.

(3) Regularize with an effective source. Unlike at first order in the mass ratio, the individual multipole modes of the second-order retarded field diverge at the particle's location. This precludes the use of the mode-sum method for regularization as it requires the multipole modes of the retarded metric perturbation to be finite at the particle's location.

The details of points 2 and 3 were fleshed out in Ref. [28] using a toy scalar-field example. In this work we address point 1 and extend our previous scalar-field results to cover Lorenz-gauge gravitational perturbations generated by a point mass on a circular orbit in a Schwarzschild background spacetime. We leave for future work the issues of extending our approach to eccentric orbits (possibly making use of methods developed for the conventional mode-sum scheme [29]) and to a Kerr background spacetime (which would likely require more extensive modification due to the common practice of using radiation gauge and spin-weighted *spheroidal* harmonics in order to achieve separability of the field equations [30,31]).

In addition to laying out a formalism that will be applicable at second order in the mass ratio, a natural by-product of this work is the extension of the standard mode-sum scheme to allow for the direct regularization of the retarded tensor modes of the metric perturbation. In the standard mode-sum procedure the retarded tensor modes of the metric perturbation must be projected onto a basis of scalar spherical harmonics before regularization can be performed. This step is cumbersome and, due to the coupling between scalar and tensor modes, requires the computation of additional tensor modes. Our new prescription neatly avoids these issues altogether.

The layout of this article is as follows. In Sec. II we outline the Lorenz-gauge field equations and their retarded solution for circular orbits in a background Schwarzschild geometry. In Sec. III we discuss the standard mode-sum and effective-source regularization procedures. In Sec. IV we detail the construction of an effective source for a Lorenz-gauge metric perturbation sourced by a particle on a circular orbit. In Sec. V we outline our numerical procedure and give our results. Finally, in Sec. VI we extend the mode-sum prescription to work directly with tensor-harmonic modes. There is additional supporting material in Appendices A–D.

This paper follows the conventions of Misner, Thorne, and Wheeler [32]; a "mostly positive" metric signature, $(-, +, +, +)$, is used for the spacetime metric, the connection coefficients are defined by $\Gamma^\lambda_{\mu\nu} = \frac{1}{2} g^{\lambda\sigma}(g_{\sigma\mu,\nu} + g_{\sigma\nu,\mu} - g_{\mu\nu,\sigma})$, the Riemann tensor is $R^\tau{}_{\lambda\mu\nu} = \Gamma^\tau_{\lambda\nu,\mu} - \Gamma^\tau_{\lambda\mu,\nu} + \Gamma^\tau_{\sigma\mu}\Gamma^\sigma_{\lambda\nu} - \Gamma^\tau_{\sigma\nu}\Gamma^\sigma_{\lambda\mu}$, the Ricci tensor and scalar are $R_{\mu\nu} = R^\tau{}_{\mu\tau\nu}$ and $R = R_\mu{}^\mu$, and the Einstein equations are $G_{\mu\nu} = R_{\mu\nu} - \frac{1}{2} g_{\mu\nu} R = 8\pi T_{\mu\nu}$. Standard geometrized units are used, with $c = G = 1$. Greek indices are used for four-dimensional spacetime components and capital latin letters are used for indices on the two-sphere. We work with standard Schwarzschild coordinates (t, r, θ, φ) and also work with a second coordinate system, (t, r, α, β), which is related by a rotation. We denote a point on the worldline of the point mass by a "0" subscript (e.g., x_0) and indices on tensors evaluated on the worldline are indicated by an overbar (e.g., $g_{\bar\mu\bar\nu}$). We also find it useful to define $f \equiv 1 - 2M/r$, where M is the mass of the background Schwarzschild black hole.

II. LORENZ-GAUGE FIELD EQUATIONS AND THEIR RETARDED SOLUTION FOR A CIRCULAR ORBIT

In this section we overview the Lorenz-gauge field equations for linear-in-the-mass-ratio perturbations of Schwarzschild spacetime, along with their decomposition into tensor-harmonic and frequency modes. The basis of tensor-harmonic modes we use is that of Barack and Sago [33,34], which are themselves a modification of the basis given by Barack and Lousto [35]. Barack and Sago also further decomposed the monopole and dipole field equations into the frequency-domain to side-step instabilities that occur when evolving those modes in the time domain (see Ref. [26] for a discussion of this issue). Later, the frequency decomposition was given for all modes with calculations for generic bound orbits by Akcay *et al.* [36,37] and Osburn *et al.* [38].

A. Field equations

Let us denote by g the full spacetime metric, which we shall consider to be the sum of the metric perturbation, h, and the background Schwarzschild metric, $\overset{\circ}{g}$, such that $g = \overset{\circ}{g} + h$. Hereafter an over-ring will denote a quantity defined with respect to the background (vacuum) spacetime. In a given coordinate system, the Einstein field equations will then take the form

$$G_{\mu\nu}[\overset{\circ}{g}_{\mu\nu} + h_{\mu\nu}] = 8\pi T_{\mu\nu} \qquad (2.1)$$

where G is the Einstein tensor, a functional of the full spacetime metric g, and T is the stress-energy tensor. Let us define the trace of the metric perturbation by $\mathrm{Tr}(h) = \overset{\circ}{g}^{\mu\nu} h_{\mu\nu}$. We shall find that the field equations for the metric perturbation take a simpler form when expressed in terms of the trace-reversed metric perturbation, $\bar{h}_{\mu\nu}$, defined by

$$\bar{h}_{\mu\nu} \equiv h_{\mu\nu} - \frac{1}{2}\overset{\circ}{g}_{\mu\nu}\mathrm{Tr}(h), \qquad (2.2)$$

so named because $\mathrm{Tr}(\bar{h}) = -\mathrm{Tr}(h)$.

As discussed in the Introduction, when we approach a second-order-in-the-mass-ratio calculation we will want to work in the Lorenz gauge. Consequently, to develop the necessary techniques we will work in the Lorenz gauge with the first-order-in-the-mass-ratio calculation we present in this work. The Lorenz-gauge condition is defined by

$$\overset{\circ}{\nabla}_{\mu}\bar{h}^{\mu\nu} = 0, \qquad (2.3)$$

where the covariant derivative is taken with respect to the background metric. By expanding the Einstein tensor in powers of the mass ratio and only retaining terms linear in μ

we arrive at the (Lorenz-gauge) linearized Einstein equation given by

$$\overset{\circ}{\Box}\bar{h}_{\mu\nu} + 2\overset{\circ}{R}{}^{\rho}{}_{\mu}{}^{\sigma}{}_{\nu}\bar{h}_{\rho\sigma} = -16\pi T_{\mu\nu} \qquad (2.4)$$

where $\overset{\circ}{\Box} = \overset{\circ}{\nabla}_{\mu}\overset{\circ}{\nabla}{}^{\mu}$ and $\overset{\circ}{R}$ is the Riemann tensor of the background spacetime. In this work we shall take the metric perturbation to be sourced by a point particle of mass μ. The corresponding energy-momentum tensor is given by

$$T_{\mu\nu} = \mu \int_{-\infty}^{\infty} [-\det(\overset{\circ}{g})]^{-1/2}\delta^4(x^{\mu} - x_0^{\mu})u_{\mu}u_{\nu}d\tau, \qquad (2.5)$$

where $\det(\overset{\circ}{g}) = r^4\sin^2\theta$ is the determinant of the background metric tensor, u^{μ} is the particle's four-velocity and τ is the proper time measured along the particle's worldline. We also use x^{μ} to denote a general spacetime coordinate and hereafter adopt the notation that a subscript "0" denotes a quantity's value evaluated at the particle. Note that for a circular orbit in the equatorial plane of a Schwarzschild black hole we have $u_r = u_\theta = 0$ and $u_t = -E_0$, $u_\varphi = L_0$, where

$$E_0 = f_0\sqrt{\frac{r_0}{r_0 - 3M}}, \qquad L_0 = r_0\sqrt{\frac{M}{r_0 - 3M}} \qquad (2.6)$$

are the (specific) orbital energy and angular momentum, respectively. Finally, we mention that the gauge equation (2.3) and field equation (2.4) are consistent so long as the particle is moving along a geodesic of the background spacetime (as then $\nabla_{\mu}T^{\mu\nu} = 0$).

The field equation in the form of Eq. (2.4) is not well suited to a numerical treatment as the metric perturbation diverges in the vicinity of the worldline. Instead, an effective-source approach can be employed to regularize the field equation and allow for a certain regular field to be solved for directly. Alternatively, with a $1 + 1$-dimensional or frequency-domain decomposition the individual multipole modes of the metric perturbation become finite at the particle's location and the mode-sum scheme can be employed to regularize on a mode-by-mode basis; see Sec. III below for an overview of these two regularization procedures. As discussed in the Introduction, at second order it will become necessary to employ an effective-source scheme even within a multipole decomposition. For that reason, despite not being required for a first-order-in-the-mass-ratio calculation, we will pursue an effective-source approach within a multipole and Fourier decomposition of the field equations. We give the details of this decomposition now.

B. Decomposition into tensor-harmonic and frequency modes

In this section we overview the multipole and Fourier decomposition of the metric perturbation and source. The explicit details of this decomposition have been laid out elsewhere [36,39] and are summarized in Appendix A; here we shall just present the key results required for this work.

There are many different conventions and notations used to define a tensor-harmonic basis. In this work we use the definition chosen by Barack and Lousto [39] with the slight modification introduced by Barack and Sago [33]. The key property of the Barack-Lousto-Sago tensor harmonics is that they form a ten-dimensional basis for any second-rank, symmetric four-dimensional tensor field in Schwarzschild spacetime. This allows us to write the ten independent components of the (trace-reversed) metric perturbation in terms of the spherical-harmonic modes of ten fields, $\bar{h}^{(i)}_{\ell m}(t, r)$ for $i = 1, \ldots, 10$ via

$$\bar{h}^{(i)}_{\ell m}(t, r) = \frac{r}{\mu a^{(i)}_\ell} \int_0^{2\pi} \int_0^\pi \bar{h}_{\tau\kappa} \eta^{\tau\mu} \eta^{\kappa\nu} Y^{(i)\ell m*}_{\mu\nu} d\Omega \qquad (2.7)$$

where $d\Omega = \sin\theta d\theta d\varphi$ and the details of the tensor basis (including definitions for $Y^{(i)\ell m}_{\mu\nu}$, $\eta^{\mu\nu}$, and $a^{(i)}_\ell$) are given in Appendix A. We further decompose into Fourier-frequency modes,

$$\bar{h}^{(i)}_{\ell m}(t, r) \equiv \frac{1}{2\pi} \int_{-\infty}^\infty \bar{h}^{(i)}_{\ell m}(\omega, r) e^{-i\omega t} dt. \qquad (2.8)$$

For periodic motion the integral over frequencies reduces to a sum over discrete harmonics (hereafter modes). In particular, for a circular geodesic orbit the mode frequency is a simple overtone of the fundamental azimuthal frequency

$$\omega_m = m\Omega_\varphi, \qquad (2.9)$$

where $\Omega_\varphi \equiv d\varphi_0/dt = \sqrt{M/r_0^3}$ and m is the azimuthal mode index. In the remainder of this article, we can therefore denote the modes by $\bar{h}^{(i)}_{\ell m}(r)$ without any ambiguity. The stress-energy tensor can be similarly decomposed into modes $T^{(i)}_{\ell m}(r)$ [35].

Substituting the mode expansions of $\bar{h}_{\mu\nu}$ and $T_{\mu\nu}$ into the linearized Einstein equation (2.4), the angular and time dependence decouples. The spherical symmetry of the background geometry ensures that the individual multipole modes are eigenfunctions of the wave operator (2.4) and consequently each multipole mode can be solved for independently from the others, though in general the ten tensorial components of each mode remain coupled. The resulting set of ordinary differential equations for each multipole mode are given by

$$\Box^{\rm sc}_{\ell m} \bar{h}^{(i)}_{\ell m} - 4f^{-2} \mathcal{M}^{(i)}_{\ (j)} \bar{h}^{(j)}_{\ell m} = \mathcal{J}^{(i)}_{\ell m} \delta(r - r_0), \qquad (2.10)$$

where $\mathcal{J}^{(i)}_{\ell m}$ comes from the decomposition of the source and $\Box^{\rm sc}_{\ell m}$ is the scalar wave operator,

$$\Box^{\rm sc}_{\ell m} = \frac{d}{dr^2} + \frac{f'}{f}\frac{d}{dr} - f^{-2}[V_\ell(r) - \omega_m^2]. \qquad (2.11)$$

Here, a prime denotes differentiation with respect to r and the potential term is given by

$$V_\ell(r) = f(r)\left[\frac{2M}{r^3} + \frac{\ell(\ell + 1)}{r^2}\right]. \qquad (2.12)$$

The $\mathcal{M}^{(i)}_{\ (j)}$ that appear in Eq. (2.10) are first-order differential operators that couple the ten components of the metric perturbation; we give their explicit form in Appendix B. In deriving the $\mathcal{M}^{(i)}_{\ (j)}$ we use in this work, we have used the frequency-domain decomposition of the Lorenz-gauge condition (2.3) to simplify the resulting equations. This decomposition of the Lorenz-gauge condition is given by

$$i\omega_m \bar{h}^{(1)} = -f\left(i\omega_m \bar{h}^{(3)} + \bar{h}^{(2)}_{,r} + \frac{\bar{h}^{(2)} - \bar{h}^{(4)}}{r}\right), \qquad (2.13)$$

$$i\omega_m \bar{h}^{(2)} = -f\bar{h}^{(1)}_{,r} + f^2\bar{h}^{(3)}_{,r} - \frac{f}{r}(\bar{h}^{(1)} - \bar{h}^{(5)} - f\bar{h}^{(3)} - 2f\bar{h}^{(6)}), \qquad (2.14)$$

$$i\omega_m \bar{h}^{(4)} = -\frac{f}{r}(r\bar{h}^{(5)}_{,r} + 2\bar{h}^{(5)} + L\bar{h}^{(6)} - \bar{h}^{(7)}), \qquad (2.15)$$

$$i\omega_m \bar{h}^{(8)} = -\frac{f}{r}(r\bar{h}^{(9)}_{,r} + 2\bar{h}^{(9)} - \bar{h}^{(10)}), \qquad (2.16)$$

where $L = \ell(\ell + 1)$.

The ten field equations (2.10) are not all coupled together; instead, they separate out into independent even- ($i = 1, \ldots, 7$) and odd-parity ($i = 8, 9, 10$) sectors. Examining the sources (given in Appendix B) we see that

$$\mathcal{J}^{(i=1,\ldots,7)} \propto [Y^{\ell m}(\pi/2, \Omega_\varphi t)]^* = 0 \quad \text{for } \ell + m = \text{odd},$$

$$\mathcal{J}^{(i=8,9,10)} \propto [Y^{\ell m}_{,\theta}(\pi/2, \Omega_\varphi t)]^* = 0 \quad \text{for } \ell + m = \text{even}.$$

Consequently we have $\bar{h}^{(i=1,\ldots,7)} = 0$ for $\ell + m = $ odd and $\bar{h}^{(i=8,9,10)} = 0$ for $\ell + m = $ even.

The gauge equations can be used to reduce the number of fields that need to be solved for simultaneously. For example, for radiative modes ($\omega_m \neq 0$) in the odd sector one can solve for the $\bar{h}^{(9)}$ and $\bar{h}^{(10)}$ fields from which the $\bar{h}^{(8)}$ field can be constructed algebraically from the gauge

TABLE I.   Hierarchical structure for solving the field equations. A "→" implies the field(s) to the right should be algebraically constructed from the fields to the left using Eqs. (2.13)–(2.16). An "(A)" implies analytic solutions are known, and we employ them in this work except in the case of the even static modes.

ℓ	m	$\ell + m =$ even	$\ell + m =$ odd
0	0	$(i) = 1, 3 \to 6$ (A)	$\cdots$
1	0	$\cdots$	$(i) = 8$ (A)
1	1	$(i) = 1, 3, 5, 6 \to 2, 4$	$\cdots$
≥ 2	0	$(i) = 1, 3, 5 \to 6, 7$ (A*)	$(i) = 8$ (A)
≥ 2	$m \neq 0$	$(i) = 1, 3, 5, 6, 7 \to 2, 4$	$(i) = 9, 10 \to 8$

equation (2.16). Similarly, for radiative modes in the even sector the number of field equations to be solved simultaneously can be reduced by using Eqs. (2.13)–(2.15). In this work we opt to only use Eqs. (2.14) and (2.15) to reduce the number of fields to be solved from seven to five. The remaining gauge equation (2.13) can then be used as a consistency check on the final result.

The static modes ($\omega_m = 0$) require a different treatment. In the odd sector both $\bar{h}^{(9)}$ and $\bar{h}^{(10)}$ are zero as their sources vanish. The resulting equation for $\bar{h}^{(8)}$ can be solved for analytically; see Ref. [35] for details. In the even sector, the gauge equations (2.14) and (2.15) can be used to eliminate the $\bar{h}^{(6)}$ and $\bar{h}^{(7)}$ fields which appear in Eqs. (B1), (B3), and (B5). The resulting set of three ordinary differential equations were first solved numerically [36], but more recently analytic solutions have been derived [38]. In this work we opt for the numerical approach.

For the nonradiative low-multipole modes ($\ell = 0, 1$, $m = 0$) analytic solutions are known [40]. The $\ell = m = 1$ mode is solved for numerically much as the other radiative even sector modes are, except for this mode $\bar{h}^{(7)} = 0$ identically. We outline this hierarchical structure for solving the field equations in Table I.

C. Retarded-field solution

In this section we outline the calculation of the retarded-field solution to Eq. (2.10) using the standard variation of parameters method. In this approach the inhomogeneous solution is constructed by multiplying the homogeneous solutions by suitable weighting coefficients. In each sector (odd/even, static/radiative) we must solve for k coupled equations and correspondingly the space of homogeneous solutions will be $2k$ dimensional. Using $j = 1, \ldots, k$ as an index for the basis of homogeneous solutions, let us define the "inner" and "outer" homogeneous solutions to the field equation by $\tilde{h}_j^{(i)-}$ and $\tilde{h}_j^{(i)+}$, respectively. The inner solutions are regular at the horizon but diverge as $r \to \infty$. Conversely, the outer solutions are regular at spatial infinity and diverge at the horizon. For the radiative modes the retarded solutions are selected by ensuring radiation at the horizon is purely ingoing and radiation at spatial infinity is

purely outgoing. This in turn implies that the asymptotic behavior of the inner and outer solutions go as

$$\tilde{h}^{(i)\pm}(r_* \to \pm\infty) \sim e^{\pm i\omega r_*}, \qquad (2.17)$$

where r_* is the tortoise radial coordinate defined by $dr_*/dr = f(r)^{-1}$. A more in-depth discussion of the asymptotic behavior of the radial fields is given in Refs. [36,37].

With the above definitions, the standard variation of parameters approach can be used to construct the inhomogeneous solutions to Eq. (2.10) via

$$\bar{h}^{(i)}(r) = \sum_{j=1}^{k} (C_j^-(r)\tilde{h}_j^{(i)-}(r) + C_j^+(r)\tilde{h}_j^{(i)+}(r)). \quad (2.18)$$

To compute the weighting coefficients $C_j^{\pm}$ we define a $2k \times 2k$ matrix of homogeneous solutions by

$$\Phi(r) = \begin{pmatrix} -\tilde{h}_j^{(i)-} & \tilde{h}_j^{(i)+} \\ -\partial_r \tilde{h}_j^{(i)-} & \partial_r \tilde{h}_j^{(i)+} \end{pmatrix}. \qquad (2.19)$$

The weighting coefficients $C_j^{\pm}(r)$ are then computed with the standard variation of parameters prescription:

$$\begin{pmatrix} C_j^-(r) \\ C_j^+(r) \end{pmatrix} = \int_a^b \Phi^{-1}(r') \begin{pmatrix} \mathbf{0} \\ \mathcal{J}^{(j)}(r')\delta(r' - r_0) \end{pmatrix} dr', \quad (2.20)$$

where the limits on the integral depend upon which weighting coefficient is being solved for. For the C_j^-'s $a = r, b = \infty$, and for the C_j^+'s $a = 2M, b = r$. The source vector is given by k zeros followed by the k sources from the right-hand side of the field equation (2.10).

The delta function in the source means the integration can be done analytically and the inhomogeneous solutions can be written explicitly as

$$\bar{h}^{(i)}(r) = \begin{cases} \sum_{j=1}^{k} C_{j0}^+ \tilde{h}_j^{(i)+}(r) & r \geq r_0, \\ \sum_{j=1}^{k} C_{j0}^- \tilde{h}_j^{(i)-}(r) & r \leq r_0, \end{cases} \quad (2.21)$$

where

$$\begin{pmatrix} C_{j0}^- \\ C_{j0}^+ \end{pmatrix} = \Phi^{-1}(r_0) \begin{pmatrix} \mathbf{0} \\ \mathcal{J}^{(j)}(r_0) \end{pmatrix}. \qquad (2.22)$$

Note that the $C_{j0}^{\pm}$ are r-independent constants.

III. REGULARIZATION

Building on the work of Mino, Sasaki, and Tanaka [6] and Quinn and Wald [7], Detweiler and Whiting showed that the gravitational self-force can be computed as the derivative of a suitable regular metric perturbation, $\bar{h}_{\mu\nu}^R$, via

$$F^{\mu}_{\text{self}}(x_0) = \mu k^{\mu\nu\gamma\delta}\nabla_{\delta}\bar{h}^{R}_{\nu\gamma}(x_0), \qquad (3.1)$$

where

$$k^{\mu\nu\gamma\delta} = \frac{1}{2}g^{\mu\delta}u^{\nu}u^{\gamma} - g^{\mu\nu}u^{\gamma}u^{\delta} - \frac{1}{2}u^{\mu}u^{\nu}u^{\gamma}u^{\delta}$$
$$+ \frac{1}{4}u^{\mu}g^{\nu\gamma}u^{\delta} + \frac{1}{4}g^{\mu\delta}g^{\nu\gamma} \qquad (3.2)$$

includes a projection operator that ensures the self-force is orthogonal to the particle's four-velocity.

The regular metric perturbation is constructed by subtracting an appropriate singular perturbation, $\bar{h}^{S}_{\mu\nu}$, from the usual retarded metric perturbation $\bar{h}^{\text{ret}}_{\mu\nu}$, i.e.,

$$\bar{h}^{R}_{\mu\nu}(x_0) = \lim_{x \to x_0}[\bar{h}^{\text{ret}}_{\mu\nu}(x) - \bar{h}^{S}_{\mu\nu}(x)]. \qquad (3.3)$$

The construction of an appropriate singular field was discussed at length in Refs. [8,41]. One of the key features of the three metric perturbations $\bar{h}^{\text{ret}/S/R}_{\mu\nu}$ is that they obey the field equations

$$\mathring{\Box}\bar{h}^{\text{ret}/S}_{\mu\nu} + 2\mathring{R}^{\rho}{}_{\mu}{}^{\sigma}{}_{\nu}\bar{h}^{\text{ret}/S}_{\rho\sigma} = -16\pi T_{\mu\nu}, \qquad (3.4)$$

$$\mathring{\Box}\bar{h}^{R}_{\mu\nu} + 2\mathring{R}^{\rho}{}_{\mu}{}^{\sigma}{}_{\nu}\bar{h}^{R}_{\rho\sigma} = 0, \qquad (3.5)$$

from which we see that the retarded and singular perturbations diverge in the same way at the particle's location,[1] while their difference—the regular perturbation—is smooth there. Using Eqs. (3.1) and (3.3), we can write the self-force as

$$F^{\mu}_{\text{self}}(x_0) = \mu\lim_{x \to x_0}[k^{\mu\nu\gamma\delta}\mathring{\nabla}_{\delta}(\bar{h}^{\text{ret}}_{\nu\gamma}(x) - \bar{h}^{S}_{\nu\gamma}(x))]$$
$$= \lim_{x \to x_0}[F^{\mu}_{\text{ret}}(x) - F^{\mu}_{S}(x)], \qquad (3.6)$$

where

$$F^{\mu}_{\text{ret}/S}(x) \equiv \mu k^{\mu\nu\gamma\delta}\mathring{\nabla}_{\delta}\bar{h}^{\text{ret}/S}_{\nu\gamma}(x). \qquad (3.7)$$

The divergence of $\bar{h}^{\text{ret}/S}_{\mu\nu}$ at the particle makes it challenging to work with Eq. (3.6) directly. Consequently, a number of reformulations have been devised to allow the gravitational self-force to be computed. Two of these schemes—the mode-sum method and the effective-source approach—we discuss now.

---

[1]Note that the retarded and singular perturbations are a solution of the same equation, but with different boundary conditions. As a result, it is only their local, singular behavior that agrees.

A. Mode-sum method

The key observation behind the mode-sum method is that although the full retarded and singular metric perturbations are divergent at the particle, their individual multipole modes remain finite everywhere. The subtraction between the retarded and singular contributions in Eq. (3.6) can then be made on a mode-by-mode basis. Explicitly, we can write

$$F^{\mu}_{\text{self}}(x_0) = \lim_{x \to x_0}\sum_{\hat{\ell}=0}^{\infty}[F^{\mu\hat{\ell}}_{\text{ret}}(x) - F^{\mu\hat{\ell}}_{S}(x)], \qquad (3.8)$$

where a superscript $\hat{\ell}$ denotes a quantity's decomposition into *scalar* spherical-harmonic modes and summed over m, i.e.,

$$F^{\mu\hat{\ell}}_{\text{ret}/S} = \sum_{m=-\hat{\ell}}^{\hat{\ell}} Y_{\hat{\ell}m}(\pi/2, \varphi_0)\int_0^{2\pi}\int_0^{\pi} F^{\mu}_{\text{ret}/S}Y^*_{\hat{\ell}m}(\theta, \varphi)d\Omega. \qquad (3.9)$$

We discuss below how we interface the tensor-mode computation of the retarded field outlined in Sec. II C and the standard mode-sum scheme we are outlining now.

The individual multipole modes of the retarded and singular contributions to the self-force $F^{(\text{ret}/S)\hat{\ell}}$ are C^{-1}. That is, they are finite at the particle but, in general, their sided limits $r \to r_0^{\pm}$ yield two different values, which we denote by $F^{\mu\hat{\ell}\pm}_{\text{ret}/S}$, respectively. For circular orbits there is no closed-form analytic solution for F^{μ}_{ret}, and typically it is computed numerically. The singular field, on the other hand, is amenable to an analytic treatment. The local structure of the singular field was first analyzed by Mino *et al.* [6] and Barack and Ori used these results to develop the mode-sum scheme shortly thereafter [21].

The scalar-harmonic mode-sum regularization formulas for the redshift invariant $h^R_{uu} \equiv h^R_{\mu\nu}u^{\mu}u^{\nu}$ [13] and for the self-force are given by

$$h^R_{uu} = \sum_{\hat{\ell}=0}^{\infty}(h^{(\text{ret})\hat{\ell}}_{\mu\nu}u^{\mu}u^{\nu} - H^{[0]}) - D_H, \qquad (3.10)$$

$$F^{\mu}_{\text{self}} = \sum_{\hat{\ell}=0}^{\infty}(F^{\mu\hat{\ell}\pm}_{\text{ret}} - F^{\mu\pm}_{[-1]}(2\hat{\ell}+1) - F^{\mu}_{[0]}) - D^{\mu}. \qquad (3.11)$$

The $\hat{\ell}$-independent $H^{[0]}, F^{\mu\pm}_{[-1]}, F^{\mu}_{[0]}, D_H, D_{\mu}$ are known as regularization parameters and their value is known for generic geodesic orbits in Schwarzschild [42] and Kerr spacetimes [43]. In general the coefficients of odd negative powers of $\hat{\ell}$ in the mode-sum formula are zero [44] and in the Lorenz gauge $D^{\mu} = D_H = 0$. For circular orbits the other nonzero regularization parameters are given by

$$H^{[0]} = \frac{4\mu}{\pi\sqrt{r_0^2 + L_0^2}}\mathcal{K}, \qquad (3.12)$$

$$F_{[-1]}^{r\pm} = \mp\frac{\mu^2}{2r_0^2}\left(1 - \frac{3M}{r_0}\right)^{1/2}, \qquad (3.13)$$

$$F_{[0]}^{r} = \frac{\mu^2 r_0 E_0^2}{\pi(L_0^2 + r_0^2)^{3/2}}[\mathcal{E} - 2\mathcal{K}], \qquad (3.14)$$

where $\mathcal{K} \equiv \int_0^{\pi/2}(1 - \frac{M}{r_0-2M}\sin^2 x)^{-1/2}dx$ and $\mathcal{E} \equiv \int_0^{\pi/2}(1 - \frac{M}{r_0-2M}\sin^2 x)^{1/2}dx$ are complete elliptic integrals of the first and second kind, respectively.

The series in $\hat{\ell}$ in both Eqs. (3.10) and (3.11) is truncated at $\hat{\ell}^{-1}$. This is sufficient to regularize h_{uu} and F^r, but the resulting sum over $\hat{\ell}$ converges rather slowly, with each term going as $\hat{\ell}^{-2}$. It is possible to derive higher-order regularization parameters [44]; Ref. [45] provides the next two nonzero parameters that serve to increase the rate of convergence of the mode sum to $\hat{\ell}^6$. It is common practice in mode-sum calculations to numerically fit for the yet higher-order unknown parameters to further increase the rate of convergence of the mode sum.

Last, as we mentioned above, we compute the retarded metric perturbation within a tensor-harmonic decomposition, whereas the standard mode-sum approach requires the retarded metric perturbation decomposed into scalar-harmonic modes as input. Thus before regularizing we must project the tensor-harmonic modes of the metric perturbation onto a basis of scalar harmonics. The projection equation takes the form

$$F_{\text{ret}}^{\mu\hat{\ell}\pm} = \frac{\mu^2}{r_0^2}\sum_{m=-\hat{\ell}}^{\hat{\ell}}\sum_{p=-3}^{3} Y^{\hat{\ell}m}(\pi/2, \varphi_p)\mathcal{F}_{(p)\pm}^{\mu,\hat{\ell}+p,m}, \qquad (3.15)$$

where the details of the $\mathcal{F}_{(p)\pm}^{\mu,\hat{\ell}+p,m}$ (but not the self-force obtained after summing over ℓ) depends on the way in which the definition for the force (a quantity which is defined *on* the worldline) is extended *off* the worldline to the whole two-sphere. Barack and Sago [33] made the computationally convenient choice for k^{abcd} where u^a has a constant value on the two-sphere, and the metric has its usual tensorial value. Their expressions for the $\mathcal{F}_{(p)\pm}^{\mu,\hat{\ell}+p,m}$ are rather cumbersome so we do not give them here; instead, their explicit form can be found in Appendix C of Ref. [33]. Likewise, a similar formula can be derived for h_{uu} [46].

The sum over p in Eq. (3.15) means that in order to compute the self-force by regularizing $\hat{\ell}_{\text{max}}$ scalar-harmonic modes one must compute $(\ell_{\text{max}} + 3)$ tensor-harmonic modes. Similarly for h_{uu} one must compute $(\ell_{\text{max}} + 2)$ tensor modes. In Sec. VI below we will recast the standard mode-sum formula to use tensor modes rather than scalar modes, which will avoid this projection step altogether.

B. Effective-source approach

The effective-source approach is an alternative practical regularization scheme for handling the divergence of the retarded field. Rather than first computing the retarded field and then subtracting the singular piece as a post-processing step, as in the mode-sum scheme, one can instead work directly with an equation for the regular field. This idea was first proposed in Refs. [22,23] and has the distinct advantage of involving only regular quantities, making it applicable in a wider variety of scenarios than the mode-sum scheme.

Using Eq. (3.3) to rewrite $\bar{h}_{\mu\nu}^{\text{ret}}$ in terms of $\bar{h}_{\mu\nu}^{R}$ and $\bar{h}_{\mu\nu}^{S}$, we can rewrite Eq. (2.4) as

$$\overset{\circ}{\Box}\bar{h}_{\mu\nu}^{R} + 2\overset{\circ}{R}{}^{\rho}{}_{\mu}{}^{\sigma}{}_{\nu}\bar{h}_{\rho\sigma}^{R} = -16\pi T_{\mu\nu} - \overset{\circ}{\Box}\bar{h}_{\mu\nu}^{S} - 2\overset{\circ}{R}{}^{\rho}{}_{\mu}{}^{\sigma}{}_{\nu}\bar{h}_{\rho\sigma}^{S}. \quad (3.16)$$

If $\bar{h}_{\mu\nu}^{S}$ is precisely the Detweiler-Whiting singular metric perturbation, then the two terms on the right-hand side of this equation cancel and $\bar{h}_{\mu\nu}^{R}$ becomes a homogeneous solution of the wave equation. However, one typically does not have access to an exact expression for $\bar{h}_{\mu\nu}^{S}$ as the Detweiler-Whiting singular metric perturbation is defined through a Hadamard parametrix [47,48] which is not even globally defined. Instead, the best one can typically do is a local expansion which is valid only in the vicinity of the worldline. Let us denote such an approximation to $\bar{h}_{\mu\nu}^{S}$ by $\bar{h}_{\mu\nu}^{P}$. With the latter we will construct an *effective source* that will allow us to directly compute the regular field at the worldline.

The puncture field $\bar{h}_{\mu\nu}^{P}$ is only valid near the worldline and so, to avoid ambiguities in the definition of the effective source, one must ensure that the puncture field goes to zero far from the particle. This is can be achieved by multiplying $\bar{h}_{\mu\nu}^{P}$ by a window function, $\mathcal{W}$, with properties such that multiplying it by $\bar{h}_{\mu\nu}^{P}$ only modifies terms of higher order in the local expansion about the worldline than those which are explicitly given in $\bar{h}_{\mu\nu}^{P}$. In our particular case, it suffices to choose $\mathcal{W}$ such that $\mathcal{W}(x_0) = 1$, $\mathcal{W}'(x_0) = 0$, $\mathcal{W}''(x_0) = 0$, and $\mathcal{W} = 0$ far away from the worldline. The residual metric perturbation $\bar{h}_{\mu\nu}^{\text{res}}$ then obeys

$$\overset{\circ}{\Box}\bar{h}_{\mu\nu}^{\text{res}} + 2\overset{\circ}{R}{}^{\rho}{}_{\mu}{}^{\sigma}{}_{\nu}\bar{h}_{\rho\sigma}^{\text{res}} = S_{\text{eff}}, \qquad (3.17)$$

where the effective source is given by

$$S_{\text{eff}} \equiv -16\pi T_{\mu\nu} - \overset{\circ}{\Box}(\mathcal{W}\bar{h}_{\mu\nu}^{P}) - 2\overset{\circ}{R}{}^{\rho}{}_{\mu}{}^{\sigma}{}_{\nu}(\mathcal{W}\bar{h}_{\rho\sigma}^{P}). \quad (3.18)$$

This effective source is smooth and finite everywhere, except on the worldline where it has limited differentiability. The corresponding residual field has the properties

$$\bar{h}_{\mu\nu}^{\text{res}}(x_0) = \bar{h}_{\mu\nu}^{R}(x_0), \qquad \nabla_\delta \bar{h}_{\mu\nu}^{\text{res}}(x_0) = \nabla_\delta \bar{h}_{\mu\nu}^{R}(x_0),$$

$$\bar{h}_{\mu\nu}^{\text{res}}(x) = \bar{h}_{\mu\nu}^{\text{ret}}(x) \quad \text{for } x \notin \text{supp}(\mathcal{W}). \qquad (3.19)$$

As the residual metric perturbation coincides with the retarded metric perturbation far from the particle, we can use the usual retarded metric perturbation boundary conditions when solving Eq. (3.17).

IV. EFFECTIVE SOURCE IN THE FREQUENCY DOMAIN

A. Construction of the puncture fields

1. Coordinate expansion of the singular field

At the core of our calculation is an effective source for the field equations which is constructed from an approximation to the Detweiler-Whiting singular field. A suitable covariant expansion of the singular field is given by

$$\bar{h}_{ab}^{(\text{S})} = 4\mu g_a{}^{\bar{a}} g_b{}^{\bar{b}} \left[\frac{1}{\epsilon} \frac{u_{\bar{a}} u_{\bar{b}}}{\bar{s}} + \mathcal{O}(\epsilon) \right], \qquad (4.1)$$

where ϵ is an order-counting parameter, $\bar{s} \equiv (g_{\bar{a}\bar{b}} + u_{\bar{a}} u_{\bar{b}}) \sigma^{\bar{a}} \sigma^{\bar{b}}$, $u^{\bar{a}}$ is the four-velocity, and $g_{\bar{a}\bar{b}}$ is the background metric, with both defined as tensors on the worldline (i.e., at the spacetime point x_0). We have also introduced the bivector of parallel transport $g_a{}^{\bar{a}}(x, x_0)$ and the Synge world function $\sigma(x, x_0)$, both of which are functions of the worldline point x_0 and the point where the singular field is to be evaluated, x.

This approximation is sufficient to produce a residual field which is finite on the worldline and which gives the correct, regularized self-force. Several higher-order terms in this expansion are also known [45] and can be incorporated into the calculation in order to accelerate convergence. However, for clarity we illustrate the approach with this simple low-order approximation and note that the methodology does not fundamentally change at higher orders.

We now wish to use the approximation (4.1) as a starting point to compute the puncture fields $\bar{h}_{\ell m}^{(i)\text{P}}$. To this end, we follow previous regularization strategies [44,45,49–52] by introducing a Riemann normal coordinate system in the vicinity of the worldline, and rewrite Eq. (4.1) as a coordinate expansion in terms of these coordinates. Specifically, we assume that the spacetime can be represented in terms of a spherical coordinate system with polar and azimuthal coordinates α and β, radius r, and time t. Note that, although our focus here is on the Schwarzschild spacetime, the assumption of a spherical coordinate system does not necessarily limit us to spherical symmetry; for example, the method works equally well in the nonspherically symmetric Kerr spacetime [52].

Now, orienting our coordinate system such that the worldline is instantaneously at $\alpha = 0$, we define the

Riemann normal coordinates $w_1 = 2 \sin \frac{\alpha}{2} \cos \beta$ and $w_2 = 2 \sin \frac{\alpha}{2} \sin \beta$. Using coordinate expansions of $g_a{}^{\bar{a}}(x, x_0)$ and $\sigma(x, x_0)$ about $x = x_0$ to linear order in $x - x_0$, we obtain an approximation to Eq. (4.1) in terms of the (t, r, w_1, w_2) Riemann normal coordinate system. Structurally, our coordinate expansion has the form

$$\bar{h}_{ab}^{(\text{S})} = \frac{1}{\epsilon} \frac{c_{ab}^{(1)}}{\rho} + \epsilon^0 \left[\frac{c_{ab}^{(2)} \Delta r}{\rho} + \frac{c_{ab}^{(3)} \Delta r^3}{\rho^3} \right] + \mathcal{O}(\epsilon), \qquad (4.2)$$

where ρ is the leading-order term in the coordinate expansion of $\bar{s}$ and the coefficients $c_{ab}^{(1)}$, $c_{ab}^{(2)}$, and $c_{ab}^{(3)}$ do not depend on Δr or α (and hence w_1 and w_2).[2] The coefficients are also independent of t since we have chosen $\Delta t = 0$, i.e., x and x_0 are points on the same time slice. There is still a potential time dependence, however, through the dependence of the coefficients on the worldline and four-velocity.

In the next subsection, we will seek a decomposition into spherical-harmonic modes. We therefore apply the (approximate) Jacobian from (w_1, w_2) coordinates to (α, β) coordinates. In doing so, we pull out a factor of $\sin \alpha$ from the Jacobian when computing $h_{t\beta}$, $h_{r\beta}$, and $h_{\alpha\beta}$, and a factor of $\sin^2 \alpha$ when computing $h_{\beta\beta}$. The reason for doing so will become clear during the mode decomposition, and is related to the fact that the Riemann normal coordinate system is regular on the worldline, but the (α, β) coordinate system is not.

Evaluating Eq. (4.1) for our particular case of a circular orbit in Schwarzschild spacetime, we arrive at our desired coordinate expansion of the Detweiler-Whiting singular metric perturbation. With Riemann normal components given by

$$\bar{h}_{tw_1} = -\frac{1}{\rho} \left[\frac{4 r_0^2 \Omega_\varphi (r_0 - 2M)}{r_0 - 3M} + \frac{2\Delta r r_0 \Omega_\varphi}{r_0 - 3M} \right. \\ \left. \times \frac{r_0^2 - 3M r_0 + 2M^2 - 2M^2 \sin^2 \beta}{(r_0 - 2M)(1 - \frac{M}{r_0 - 2M} \sin^2 \beta)} \right], \qquad (4.3a)$$

$$\bar{h}_{rw_1} = \frac{4M r_0 \sin \alpha \cos \beta}{\rho (r_0 - 3M)}, \qquad (4.3b)$$

$$\bar{h}_{w_1 w_1} = \frac{\cos^2 \beta}{\rho} \left[\frac{4M r_0^2}{r_0 - 3M} + \frac{2\Delta r M r_0}{r_0 - 3M} \right. \\ \left. \times \frac{3r_0 - 7M - 2M \sin^2 \beta}{(r_0 - 2M)(1 - \frac{M}{r_0 - 2M} \sin^2 \beta)} \right], \qquad (4.3c)$$

---

[2]This form is valid for the case of circular orbits in Schwarzschild spacetime, where any quadratic dependence on w_1 and w_2 can be replaced with a term involving ρ^2 and Δr^2. The structure is slightly more complicated in more general cases where odd powers of w_1 and w_2 can appear, but nonetheless the following analysis remains qualitatively unchanged.

TABLE II. Integrands appearing in the mode decomposition of all ten tensor-harmonic components of the singular metric perturbation for the case of a circular geodesic orbit in Schwarzschild spacetime.

(i, ℓ, m')	Integrand
$(1, \ell, 0)$	$r\sqrt{\frac{2\ell+1}{4\pi}}(\bar{h}_{tt} + f^2\bar{h}_{rr})P_\ell^0(\cos\alpha)\sin\alpha$
$(2, \ell, \pm1)$	$\pm 2r\sqrt{\frac{2\ell+1}{4\pi\ell(\ell+1)}}f\bar{h}_{tr}\cos\beta\,P_\ell^1(\cos\alpha)\sin\alpha$
$(3, \ell, 0)$	$r\sqrt{\frac{2\ell+1}{4\pi}}f(\bar{h}_{tt} - f^2\bar{h}_{rr})P_\ell^0(\cos\alpha)\sin\alpha$
$(4, \ell, \pm1)$	$\pm 2\sqrt{\frac{(2\ell+1)\ell(\ell+1)}{4\pi}}\frac{\bar{h}_{tw_1}}{\ell(\ell+1)}\left[\sin^2\beta\,P_\ell^1(\cos\alpha) + \cos^2\beta\frac{\ell^2 P_{\ell+1}^1(\cos\alpha)-(\ell+1)^2 P_{\ell-1}^1(\cos\alpha)}{2\ell+1}\right]$
$(5, \ell, 0)$	$2\sqrt{\frac{2\ell+1}{4\pi}}f\bar{h}_{rw_1}\cos\beta\frac{\ell(\ell+1)}{2\ell+1}\left[P_{\ell+1}^0(\cos\alpha) - P_{\ell-1}^0(\cos\alpha)\right]$
$(5, \ell, \pm2)$	$2\sqrt{\frac{(2\ell+1)\ell(\ell+1)}{4\pi(\ell-1)(\ell+2)}}f\bar{h}_{rw_1}\cos\beta\frac{1}{\ell(\ell+1)}\left[4\sin^2\beta\,P_\ell^2(\cos\alpha) + (\cos^2\beta - \sin^2\beta)\frac{(\ell-1)\ell P_{\ell+1}^2(\cos\alpha)-(\ell+1)(\ell+2)P_{\ell-1}^2(\cos\alpha)}{2\ell+1}\right]$
$(6, \ell, 0)$	$\frac{1}{r}\sqrt{\frac{2\ell+1}{4\pi}}\bar{h}_{w_1w_1}P_\ell^0(\cos\alpha)\sin\alpha$
$(7, \ell, \pm2)$	$\frac{2}{r}\sqrt{\frac{(2\ell+1)(\ell-1)\ell(\ell+1)(\ell+2)}{4\pi}}\frac{1}{(\ell-1)\ell(\ell+1)(\ell+2)}\frac{\bar{h}_{w_1w_1}}{\sin\alpha}\left[8\cos^2\beta\sin^2\beta\frac{(\ell-1)^2 P_{\ell+1}^2(\cos\alpha)-(\ell+2)^2 P_{\ell-1}^2(\cos\alpha)}{2\ell+1}\right.$
	$\left.+(\cos^2\beta - \sin^2\beta)^2\frac{(\ell-1)^2\ell^2(2\ell-1)P_{\ell+2}^2(\cos\alpha)-2(\ell-3)(\ell-1)(\ell+2)(\ell+4)(2\ell+1)P_\ell^2(\cos\alpha)+(\ell+1)^2(\ell+2)^2(2\ell+3)P_{\ell-2}^2(\cos\alpha)}{2(2\ell-1)(2\ell+1)(2\ell+3)}\right]$
$(8, \ell, \pm1)$	$-2\sqrt{\frac{(2\ell+1)\ell(\ell+1)}{4\pi}}\frac{i\bar{h}_{tw_1}}{\ell(\ell+1)}\left[P_\ell^1(\cos\alpha)\cos^2\beta + \frac{\ell^2 P_{\ell+1}^1(\cos\alpha)-(\ell+1)^2 P_{\ell-1}^1(\cos\alpha)}{2\ell+1}\sin^2\beta\right]$
$(9, \ell, \pm2)$	$\mp\sqrt{\frac{(2\ell+1)\ell(\ell+1)}{4\pi(\ell-1)(\ell+2)}}4if\bar{h}_{rw_1}\cos\beta\frac{1}{\ell(\ell+1)}\left[(\cos^2\beta - \sin^2\beta)P_\ell^2(\cos\alpha) + \sin^2\beta\frac{(\ell-1)\ell P_{\ell+1}^2(\cos\alpha)-(\ell+1)(\ell+2)P_{\ell-1}^2(\cos\alpha)}{2\ell+1}\right]$
$(10, \ell, \pm2)$	$\mp\frac{1}{r}\sqrt{\frac{(2\ell+1)(\ell-1)\ell(\ell+1)(\ell+2)}{4\pi}}\frac{1}{(\ell-1)\ell(\ell+1)(\ell+2)}\frac{4i\bar{h}_{w_1w_1}}{\sin\alpha}\left[(\cos^2\beta - \sin^2\beta)^2\frac{(\ell-1)^2 P_{\ell+1}^2(\cos\alpha)-(\ell+2)^2 P_{\ell-1}^2(\cos\alpha)}{2\ell+1}\right.$
	$\left.+\cos^2\beta\sin^2\beta\frac{(\ell-1)^2\ell^2(2\ell-1)P_{\ell+2}^2(\cos\alpha)-2(\ell-3)(\ell-1)(\ell+2)(\ell+4)(2\ell+1)P_\ell^2(\cos\alpha)+(\ell+1)^2(\ell+2)^2(2\ell+3)P_{\ell-2}^2(\cos\alpha)}{(2\ell-1)(2\ell+1)(2\ell+3)}\right]$

our approximation to the Detweiler-Whiting singular metric is then given by

$$\bar{h}_{tt} = \frac{1}{\rho}\left[\frac{4(r_0-2M)^2}{r_0(r_0-3M)} - \frac{2\Delta r}{r_0^2(r_0-3M)}\right.$$
$$\left.\times\frac{r_0^2 - 7Mr_0 + 10M^2 - 2M(r_0-4M)\sin^2\beta}{1 - \frac{M}{r_0-2M}\sin^2\beta}\right], \quad (4.4\text{a})$$

$$\bar{h}_{tr} = -\frac{4r_0\Omega_\varphi(r_0-2M)\sin\alpha\cos\beta}{\rho(r_0-3M)}, \quad (4.4\text{b})$$

$$\bar{h}_{t\alpha} = \bar{h}_{tw_1}\cos\beta, \quad (4.4\text{c})$$

$$\bar{h}_{t\beta} = -\bar{h}_{tw_1}\sin\alpha\sin\beta, \quad (4.4\text{d})$$

$$\bar{h}_{rr} = 0, \quad (4.4\text{e})$$

$$\bar{h}_{r\alpha} = \bar{h}_{rw_1}\cos\beta, \quad (4.4\text{f})$$

$$\bar{h}_{r\beta} = -\bar{h}_{rw_1}\sin\alpha\sin\beta, \quad (4.4\text{g})$$

$$\bar{h}_{\alpha\alpha} = \bar{h}_{w_1w_1}\cos^2\beta, \quad (4.4\text{h})$$

$$\bar{h}_{\alpha\beta} = -\bar{h}_{w_1w_1}\sin\alpha\sin\beta\cos\beta, \quad (4.4\text{i})$$

$$\bar{h}_{\beta\beta} = \bar{h}_{w_1w_1}\sin^2\alpha\sin^2\beta. \quad (4.4\text{j})$$

This approximation includes all contributions at order ϵ^{-1} and ϵ^0, with the exception of terms proportional to $\Delta r^3/\rho^3$, which we neglect as their mode decomposition yields only terms proportional to Δr^2 and higher.

2. Mode decomposition

We now proceed with the decomposition of our coordinate expansion into tensor spherical-harmonic modes. For this, we must evaluate the integrals of the singular field against the tensor spherical harmonics,

$$\bar{h}_{\ell m}^{(i)P} = \frac{r}{\mu a_\ell^{(i)}}\int_0^{2\pi}\int_0^\pi \bar{h}_{\tau\kappa}\eta^{\tau\mu}\eta^{\kappa\nu}Y_{\mu\nu}^{(i)\ell m*}\sin\alpha\,d\alpha\,d\beta. \quad (4.5)$$

For the circular orbit case we are considering here, the explicit form for the integrand for each $i = 1, \ldots, 10$ field is given in Table II.

The mode decomposition works much the same as with the scalar-field case described in Ref. [28]. There are, however, some key differences which introduce additional complexity to the gravitational case:

(1) The fact that we have tensor (as opposed to scalar) harmonics makes the mode decomposition integrals slightly more involved.

(2) Whereas in the scalar case we only required the $m' = 0$ modes, we now require $m' = 0$ for $\bar{h}_{\ell m}^{(1)}$, $\bar{h}_{\ell m}^{(3)}$, and $\bar{h}_{\ell m}^{(6)}$, $m' = 1$ for $\bar{h}_{\ell m}^{(2)}$, $\bar{h}_{\ell m}^{(4)}$, and $\bar{h}_{\ell m}^{(8)}$, $m' = 0, 2$ for $\bar{h}_{\ell m}^{(5)}$, and $m' = 2$ for $\bar{h}_{\ell m}^{(7)}$, $\bar{h}_{\ell m}^{(9)}$, and $\bar{h}_{\ell m}^{(10)}$. This is

because we would like to compute the metric perturbation and its derivative (for the self-force) on the worldline, and these are the only modes which do not vanish on the worldline at $\alpha = 0$. Note that in principle other modes could contribute ($m' = 1$ for $\bar{h}_{\ell m}^{(1)}$, $\bar{h}_{\ell m}^{(3)}$, and $\bar{h}_{\ell m}^{(6)}$, $m' = 0$ for $\bar{h}_{\ell m}^{(2)}$, $m' = 0, 2$ for $\bar{h}_{\ell m}^{(4)}$ and $\bar{h}_{\ell m}^{(8)}$, $m' = 1$ for $\bar{h}_{\ell m}^{(5)}$ and $\bar{h}_{\ell m}^{(9)}$, and $m' = 1, 3$ for $\bar{h}_{\ell m}^{(7)}$ and $\bar{h}_{\ell m}^{(10)}$), but the integrals for those modes all contain odd powers of $\sin\beta$ or $\cos\beta$ and therefore their contribution vanishes after integration over β.

(3) The coordinate approximation we are using for the singular field has a spurious nonsmoothness away from the worldline at $\alpha = \pi$. This can be seen in ρ, which has a β-direction-dependent limit as $\alpha \to \pi$. This problem did not manifest itself in the scalar case, since the isotropic nature of the $m' = 0$ mode means it cannot include any information about direction dependence.

The first two items above do not cause any fundamental issues; they merely add some extra algebraic complexity to the problem. The third item, however, does cause problems if not handled appropriately. The nonsmoothness introduces a spurious component in the puncture which behaves as $\frac{(-1)^{\ell}}{\ell}$ in a mode-sum formula such as Eqs. (3.10) and (3.11). This renders the sum not absolutely convergent, although the $(-1)^{\ell}$ factor means that it is in fact conditionally convergent since, for example, $\sum_{\ell=1}^{\infty} \frac{(-1)^{\ell+1}(2\ell+1)}{\ell(\ell+1)} = 1$. In practice, this makes the sum over modes converge very slowly; see Fig. 1.
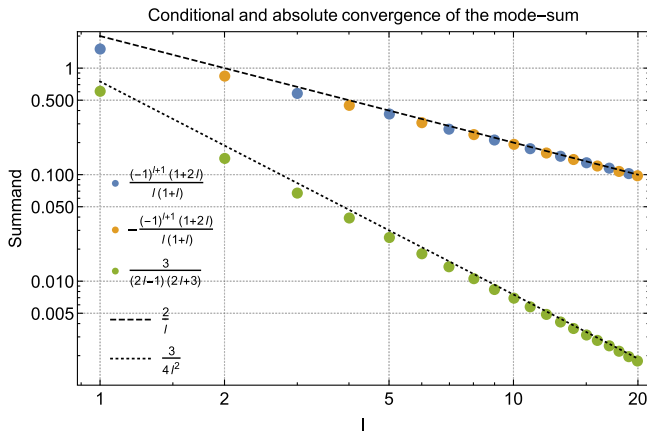

FIG. 1 (color online). Effect of a spurious nonsmoothness away from the worldline on the convergence of a mode-sum scheme near the worldline. The nonsmoothness manifests itself as a term of the form $\frac{(-1)^{\ell+1}(2\ell+1)}{\ell(\ell+1)}$ and appears to spoil any hope of rapid convergence (blue/orange dots). This can be mitigated by using a smoothing factor which converts the conditionally convergent behavior into a more rapid absolutely convergent behavior (green). The final result is not altered since the infinite sum of conditionally convergent terms is exactly equal to the infinite sum of absolutely convergent terms.

Fortunately, there is a straightforward resolution to this problem. A smooth window function $\mathcal{W}_{m'}(\alpha)$ in the α direction is effective in eliminating the spurious nonsmoothness affecting the modes. To ensure that the self-force is not affected, we require that $\mathcal{W}_{m'}(\alpha) \sim 1 + \mathcal{O}(\alpha^2)$ near $\alpha = 0$, while eliminating the effect of the nonsmoothness on a particular m' mode requires $\mathcal{W}_{m'}(\alpha) \sim (\pi - \alpha)^{\lceil m'/2 \rceil}$ near $\alpha = \pi$, where $\lceil m'/2 \rceil$ is the smallest integer greater than or equal to $m'/2$. We make the particular choice $\mathcal{W}_{m'}(\alpha) = (\cos\frac{\alpha}{2})^{\lceil m'/2 \rceil}$, which satisfies both of the above criteria.

3. Integrals over α

In the circular geodesic case, the quantity ρ appearing in the singular metric perturbation is given by

$$\rho^2 = \frac{2\chi r_0^2(r_0 - 2M)}{r_0 - 3M}(\delta^2 + 1 - \cos\alpha), \quad (4.6)$$

where

$$\delta^2 \equiv \frac{\Delta r^2}{2\chi r_0}\frac{r_0 - 3M}{(r_0 - 2M)^2} \quad (4.7)$$

and

$$\chi \equiv 1 - \frac{M}{r_0 - 2M}\sin^2\beta. \quad (4.8)$$

Then, the integrals over α all take one of nine possible forms which can be evaluated analytically. In our particular case, we are only interested in the behavior at the leading two orders in $\Delta r \equiv r - r_0$. To simplify our expressions, we introduce

$$\Lambda_1 \equiv \Lambda_{1,0} = \frac{\ell(\ell+1)}{(2\ell-1)(2\ell+3)} \quad (4.9)$$

and

$$\Lambda_2 \equiv \Lambda_{2,0} = \frac{(\ell-1)\ell(\ell+1)(\ell+2)}{(2\ell-3)(2\ell-1)(2\ell+3)(2\ell+5)}, \quad (4.10)$$

where $\Lambda_{m,n}$ is defined later in Eq. (6.3). Then, for $\bar{h}_{\ell 0}^{(1)}$, $\bar{h}_{\ell 0}^{(3)}$, and $\bar{h}_{\ell 0}^{(6)}$ the Δr-expanded integrals are given by

$$\int_0^{\pi} \frac{P_\ell^0(\cos\alpha)\sin\alpha}{(\delta^2 + 1 - \cos\alpha)^{1/2}}\,d\alpha$$
$$= \frac{1}{2\ell+1}[2\sqrt{2} - 2(2\ell+1)|\delta| + \mathcal{O}(\delta^2)]. \quad (4.11)$$

For $\bar{h}_{\ell 1}^{(2)}$ they are given by

$$\int_0^\pi \frac{P_\ell^1(\cos\alpha)\sin^2\alpha}{(\delta^2+1-\cos\alpha)^{1/2}}d\alpha = \frac{1}{2\ell+1}[-8\sqrt{2}\Lambda_1 + \mathcal{O}(\delta^2)],$$

(4.12)

For $\bar{h}_{\ell 1}^{(4)}$ and $\bar{h}_{\ell 1}^{(8)}$ they are given by

$$\int_0^\pi \frac{\mathcal{W}_1(\alpha)}{\ell(\ell+1)}\frac{\ell^2 P_{\ell+1}^1(\cos\alpha)-(\ell+1)^2 P_{\ell-1}^1(\cos\alpha)}{(2\ell+1)(\delta^2+1-\cos\alpha)^{1/2}}d\alpha$$

$$= \frac{1}{2\ell+1}\left[-\frac{6\sqrt{2}}{(2\ell-1)(2\ell+3)}+(2\ell+1)|\delta|+\mathcal{O}(\delta^2)\right]$$

(4.13)

and

$$\int_0^\pi \frac{\mathcal{W}_1(\alpha)}{\ell(\ell+1)}\frac{P_\ell^1(\cos\alpha)}{(\delta^2+1-\cos\alpha)^{1/2}}d\alpha$$

$$= \frac{1}{2\ell+1}\left[-8\sqrt{2}\Lambda_1 + \frac{6\sqrt{2}}{(2\ell-1)(2\ell+3)}\right.$$

$$\left. + (2\ell+1)|\delta|+\mathcal{O}(\delta^2)\right].$$

(4.14)

For $\bar{h}_{\ell 0}^{(5)}$ they are given by

$$\int_0^\pi \frac{\ell(\ell+1)}{(2\ell+1)}\frac{[P_{\ell+1}^0(\cos\alpha)-P_{\ell-1}^0(\cos\alpha)]\sin\alpha}{(\delta^2+1-\cos\alpha)^{1/2}}d\alpha$$

$$= \frac{1}{2\ell+1}[-8\sqrt{2}\Lambda_1 + \mathcal{O}(\delta^2)].$$

(4.15)

For $\bar{h}_{\ell 2}^{(5)}$ and $\bar{h}_{\ell 2}^{(9)}$ they are given by

$$\int_0^\pi \frac{1}{\ell(\ell+1)}\frac{\mathcal{W}_2(\alpha)P_\ell^2(\cos\alpha)\sin\alpha}{(\delta^2+1-\cos\alpha)^{1/2}}d\alpha$$

$$= \frac{1}{2\ell+1}\left[32\sqrt{2}\Lambda_2\right.$$

$$\left. - \frac{120\sqrt{2}(\ell-1)(\ell+2)}{(2\ell-3)(2\ell-1)(2\ell+3)(2\ell+5)}+\mathcal{O}(\delta^2)\right]$$

(4.16)

and

$$\int_0^\pi \frac{\mathcal{W}_2(\alpha)\sin\alpha}{(2\ell+1)\ell(\ell+1)(\delta^2+1-\cos\alpha)^{1/2}}$$

$$\times[(\ell-1)\ell P_{\ell+1}^2(\cos\alpha)-(\ell+1)(\ell+2)P_{\ell-1}^2(\cos\alpha)]d\alpha$$

$$= \frac{1}{2\ell+1}\left[-32\sqrt{2}\Lambda_2\right.$$

$$\left. + \frac{240\sqrt{2}(\ell-1)(\ell+2)}{(2\ell-3)(2\ell-1)(2\ell+3)(2\ell+5)}+\mathcal{O}(\delta^2)\right].$$

(4.17)

Finally, for $\bar{h}_{\ell 2}^{(7)}$ and $\bar{h}_{\ell 2}^{(10)}$ they are given by

$$\int_0^\pi \frac{\mathcal{W}_2(\alpha)\csc\alpha}{(\ell-1)\ell(\ell+1)(\ell+2)(2\ell+1)(\delta^2+1-\cos\alpha)^{1/2}}$$

$$\times[(\ell-1)^2 P_{\ell+1}^2(\cos\alpha)-(\ell+2)^2 P_{\ell-1}^2(\cos\alpha)]d\alpha$$

$$= \frac{1}{2\ell+1}\left[\frac{10\sqrt{2}}{(2\ell-1)(2\ell+3)}-\frac{1}{4}(2\ell+1)|\delta|+\mathcal{O}(\delta^2)\right]$$

(4.18)

and

$$\int_0^\pi \frac{1}{(\ell-1)\ell(\ell+1)(\ell+2)}$$

$$\times \frac{\mathcal{W}_2(\alpha)\csc\alpha}{(\delta^2+1-\cos\alpha)^{1/2}}\frac{1}{(2\ell-1)(2\ell+1)(2\ell+3)}$$

$$\times[(\ell-1)^2\ell^2(2\ell-1)P_{\ell+2}^2(\cos\alpha)$$

$$- 2(\ell-3)(\ell-1)(\ell+2)(\ell+4)(2\ell+1)P_\ell^2(\cos\alpha)$$

$$+ (\ell+1)^2(\ell+2)^2(2\ell+3)P_{\ell-2}^2(\cos\alpha)]d\alpha$$

$$= \frac{1}{2\ell+1}\left[-32\sqrt{2}\Lambda_2 + \frac{40\sqrt{2}}{(2\ell-1)(2\ell+3)}\right.$$

$$\left. + (2\ell+1)|\delta|+\mathcal{O}(\delta^2)\right].$$

(4.19)

4. Integrals over β

With the integrals over α having been evaluated analytically as a power series in δ, we are next faced with the integrals over β. The functional dependence on β can be rewritten in terms of integer and half-integer powers of $\chi = 1 - \frac{M}{r_0-2M}\sin^2\beta$. These integrals are straightforward to evaluate and yield either polynomials in $\frac{M}{r_0-2M}$, or complete elliptic integrals with argument $\frac{M}{r_0-2M}$. Specifically,

$$\int_0^{2\pi}\chi^n d\beta = 2\pi\,_2F_1\left(n,\frac{1}{2},1,\frac{M}{r_0-2M}\right),$$

(4.20)

which has three special cases: for $n=-1/2$ it reduces to the elliptic integral of the first kind, $\mathcal{K}(\frac{M}{r_0-2M})$; for $n=1/2$ it reduces to the elliptic integral of the second kind, $\mathcal{E}(\frac{M}{r_0-2M})$; for n an integer it is a polynomial in $\frac{M}{r_0-2M}$. All other cases can be related to these three using the recursion relation for the hypergeometric function,

$$\mathcal{F}_{p+1}(k) = \frac{p-1}{p(k-1)}\mathcal{F}_{p-1}(k) + \frac{1-2p+(p-\frac{1}{2})k}{p(k-1)}\mathcal{F}_p(k),$$

(4.21)

where $\mathcal{F}_p(k) \equiv\,_2F_1(p,\frac{1}{2},1,k)$.

B. Construction of the effective source and residual fields

In order to construct an effective source we must choose a window function $\mathcal{W}$ to confine the definition of the puncture to a neighborhood of the worldline. As discussed in Sec. III B, the constraints on the window function are that $\mathcal{W}(x_0) = 1, \mathcal{W}'(x_0) = 0, \mathcal{W}''(x_0) = 0,$ and $\mathcal{W} = 0$ far away from the worldline. These conditions leave considerable freedom when choosing a window function. In this work we shall use the window function given by

$$\mathcal{W}(r) = e^{-8M^{-4}(r-r_0)^4}. \qquad (4.22)$$

We make this choice as it is easy to implement and, although not formally compact, it is effectively compact within our numerical scheme. Other authors have made different choices. Vega *et al.* [53] used a compact window function that allowed for a smooth transition from the residual to the retarded field. Alternatively, a compact source can be achieved using the worldtube approach of Barack and Golbourn [22]. In Ref. [28] we used a Heaviside Π function and showed that this was equivalent to the worldtube method. In this work we opt not to do this for ease of implementation, though we note (by building on a draft of this work) that a worldtube method has been implemented for the gravitational case [54].

With the window function chosen the effective sources are given by

$$S_{\ell m}^{(i)\text{eff}} = \mathcal{J}_{\ell m}^{(i)}\delta(r - r_0) - \Box_{\ell m}^{sc}(\mathcal{W}\bar{h}_{\ell m}^{(i)P})$$
$$+ 4f^{-2}\mathcal{M}^{(i)}{}_{(j)}(\mathcal{W}\bar{h}_{\ell m}^{(j)P}). \qquad (4.23)$$

For brevity we will not display the explicit form of the $S_{\ell m}^{(i)\text{eff}}$. Using the field equations in Appendix B and punctures in Appendix C, it is straightforward to compute the effective sources using computer algebra packages. However, we do point out one potential subtlety: in the above equation we have implicitly assumed that the wave operator commutes with the mode decomposition, an assumption which is not necessarily true. Indeed, Barack and Ori [49] pointed out that the mode decomposition does *not* always commute with radial derivatives; likewise, from the Wigner-Eckart theorem one may be concerned that a spherical-harmonic mode decomposition which fails to include all modes would not commute with the angular derivatives. In the current context both concerns turn out to be unfounded. The Barack-Ori observation is only an issue if the limit $\Delta r \to 0$ is taken, but we avoid doing so while computing the puncture fields. The higher spherical-harmonic modes of the puncture that we neglect would indeed contribute to the effective source one obtains, but only in a way which affects the higher derivatives of the residual field (since those higher modes vanish when evaluated at $\alpha = 0$).

The construction of the residual metric perturbation now proceeds as follows. Via the variation of parameters prescription we have

$$\bar{h}^{(i)\text{res}}(r) = \sum_{j=1}^{k}(C_j^{-\text{res}}(r)\tilde{h}_j^{(i)-}(r) + C_j^{+\text{res}}(r)\tilde{h}_j^{(i)+}(r)), \qquad (4.24)$$

where recall that we use j to index the k basis of a given ℓm mode. The weighting coefficients are given by

$$\begin{pmatrix} C_j^{-\text{res}}(r) \\ C_j^{+\text{res}}(r) \end{pmatrix} = \int_a^b \Phi^{-1}(r') \begin{pmatrix} \mathbf{0} \\ S^{(i)\text{eff}} \end{pmatrix} dr', \qquad (4.25)$$

where Φ is the $2k \times 2k$ matrix of homogeneous solutions, defined in Eq. (2.19). The source vector is formed of k zeros followed by the k effective sources. The integration limits in Eq. (4.25) depend upon which weighting coefficient is being solved for. For the $C_j^{-\text{res}}$'s $a = r, b = \infty$, and for the $C_j^{+\text{res}}$'s $a = 2M, b = r$.

In order to compute the self-force we also require the first radial derivatives of the metric perturbation fields. These are easily constructed via

$$\bar{h}^{(i)\text{res}\prime}(r) = \sum_{j=1}^{k}(C_j^{-\text{res}}(r)\tilde{h}_j^{(i)-\prime}(r) + C_j^{+\text{res}}(r)\tilde{h}_j^{(i)+\prime}(r)). \qquad (4.26)$$

Last, we discuss how to construct the remaining fields using the gauge equations and the hierarchical scheme outlined in Table I. This is achieved by noting that the gauge equations (2.13)–(2.16) are for the retarded field. On the worldline we can write $\bar{h}^{(i)} = \bar{h}^{(i)\text{res}} + \bar{h}^{(i)P}$. The remaining residual fields can be obtained by substituting this split into the gauge equations and rearranging for the $\bar{h}^{(i)\text{res}}$.

V. NUMERICAL IMPLEMENTATION AND RESULTS

The self-force experienced by a particle moving along a fixed geodesic of the background Schwarzschild spacetime was first calculated in the Lorenz gauge by Barack and Sago [33]. In calculating the retarded field they used a time-domain implementation for the $\ell \geq 2$ modes and used a frequency-domain method to calculate the monopole ($\ell = 0$) and dipole ($\ell = 1$) modes [35,40]. They constructed the self-force by projecting the tensor-harmonic modes of the retarded field onto a basis of scalar harmonics and regularizing using the standard mode-sum scheme. Lorenz-gauge calculations were later extended to generic bound orbits in Schwarzschild spacetime [34,36–38,55,56].

In this section we detail how to compute, in the frequency domain, the Lorenz-gauge self-force along a

circular geodesic using the effective-source method we have developed above. Before giving the algorithm for the computation we briefly discuss how we construct numerical boundary conditions in order to solve for the retarded homogeneous metric perturbation.

A. Numerical boundary conditions

For the radiative modes ($\omega \neq 0$) the asymptotic boundary conditions for the retarded-field solutions are given by Eq. (2.17). In practice we cannot place the boundaries of our numerical domain at $r_* = \pm\infty$. Instead we construct boundary conditions at a finite radius by expanding the asymptotic boundary conditions in an appropriate series. For the radiative modes we use the expansions

$$\tilde{h}^{(i)-}(r_{\rm in}) = e^{-i\omega_m r_*^{\rm in}} \sum_{k=0}^{k_{\max}^-} b_k^i (r_{\rm in} - 2M)^k, \qquad (5.1)$$

$$\tilde{h}^{(i)+}(r_{\rm out}) = e^{i\omega_m r_*^{\rm out}} \sum_{k=0}^{k_{\max}^+} \frac{a_k^i}{r_{\rm out}^k}, \qquad (5.2)$$

where $r_*^{\rm in/out} \equiv r_*(r_{\rm in/out})$. How the boundary locations $r_{\rm in/out}$ and the truncation values $k_{\max}^\pm$ are selected in practice will be discussed in the algorithm section below. The series coefficients a_k^i, b_k^i are found by substituting the above expansions into the field equations (2.10) and solving for the resulting recursion relations. For brevity we do not repeat these relations here; they can be found in Appendix A of Ref. [36]. The recursion relations determine the $a_{k>0}^i, b_{k>0}^i$ in terms of the first coefficients a_0^i, b_0^i, respectively. By selecting appropriate linearly independent vectors of these leading coefficients we construct a basis of linearly independent solutions that span the solution space for the field equations. For example, for the odd radiative modes we have, once the gauge equations are employed, a solution space with two degrees of freedom, i.e., we must solve for $\bar{h}^{(9)}$ and $\bar{h}^{(10)}$. For the outer homogeneous solutions the two basis are formed by setting $\{a_0^9, a_0^{10}\} = \{1, 0\}$ and $\{a_0^9, a_0^{10}\} = \{0, 1\}$. Similarly we can repeat this with $\{b_0^9, b_0^{10}\}$ for the inner solutions.

In this work, although analytic solutions are now known [38], we opt to solve for the even static modes numerically as we already have code to do so. For these modes the numerical boundary conditions take the form

$$\tilde{h}^{(i)-}(r_{\rm in}) = \sum_{k=k_{\min}^-}^{k_{\max}^-} b_k^i (r_{\rm in} - 2M)^k, \qquad (5.3)$$

$$\tilde{h}^{(i)+}(r_{\rm out}) = \sum_{k=k_{\min}^+}^{k_{\max}^+} \frac{a_k^i + \bar{a}_k^i \log r_{\rm out}}{r_{\rm out}^k}. \qquad (5.4)$$

How the truncation values $k_{\min}^\pm$ are selected and the form of the recursion relations for $a_k^i, \bar{a}_k^i, b_k^i$ is again given in Ref. [36]. The log term in Eq. (5.4) is added to ensure the recursion relations have sufficient degrees of freedom to span the space of solutions to the field equations.

B. Numerical algorithm

The following steps describe how we calculate the self-force in practice via our frequency-domain effective-source approach.

(1) Choose a radial grid to store the values of various fields on. In general we require high resolution near the particle, and lower resolution far from the particle. Though our chosen window function is not formally compact, within our numerical procedure it is effectively compact. It is inside this effectively compact region that we need high resolution. In general we choose our window function to be effectively zero outside the region ($r_0 - 2M, r_0 + 2M$). Inside this region we find a grid spacing of $M/10$ sufficient (we pick the grid so that it includes $r = r_0$). Outside the (effective) support of the window function we use a grid spacing of $2M$.

(2) For radiative modes ($m \neq 0$) and even static modes ($\ell = \text{even} \geq 2, m = 0$), construct numerical boundary conditions at $r = r_{\rm out}$ and $r = r_{\rm in}$ using the recursion relations in Appendix A of Ref. [36]. For each ℓm mode there will be n_f inhomogeneous fields to solve for (see Table I), and correspondingly n_f sets of boundary conditions for the homogeneous fields will be constructed as described in Sec. V A.

(3) For a given ℓm mode, solve for each basis of homogeneous solutions and store the values of the fields and their derivatives on the preselected radial grid points.

(4) For the odd static ($\ell = \text{odd}, m = 0$) modes and the monopole ($\ell = m = 0$) the values of the (in)homogeneous fields and their derivatives can be computed analytically. See Appendix D for an explicit overview of the calculation for the monopole mode.

(5) For the given ℓm mode, compute the effective-source vector and store the results on the radial grid.

(6) At each grid point invert the matrix of homogeneous solutions defined in Eq. (2.19) (formed from the previous stored results) and multiply it by the source vector to form the integrand of Eq. (4.25). Store the resulting values of the weighting coefficient integrands at each point on the radial grid.

(7) Interpolate the weighting coefficient integrands using standard cubic spline techniques. Numerically integrate the integrand as described by Eq. (4.25). The regular radial metric perturbation fields and their radial derivatives are then computed via Eqs. (4.24) and (4.26), respectively.

TABLE III.   Sample results for orbits with $r_0 = 6M$ and $r_0 = 10M$ computed with $\ell_{max} = 40$. The relative difference between our results and previously published data is small, being always less than 3×10^{-7}. These results were computed using the higher-order punctures available online as Supplemental Material [57], and by numerically fitting for the higher-order regularization parameters in order to speed up the convergence of the sum over tensor ℓ modes. Numbers in brackets denote the estimated error in the final digit of the corresponding result. Note that the results in this table have been adimensionalized, i.e., h_{uu}^R here $\equiv (M/\mu)h_{uu}^R$ and F^r here $\equiv (M/\mu)^2 F^r$.

	r_0/M	this work	Akcay *et al.* [18,37]	rel. diff.
h_{uu}^R	6	$-1.0471852(4)$	$-1.0471854796(1)$	2×10^{-7}
F^r	6	$2.4466487(8) \times 10^{-2}$	$2.4466495(4) \times 10^{-2}$	3×10^{-7}
h_{uu}^R	10	$-0.48925802(2)$	$-0.48925800172(4)$	4×10^{-8}
F^r	10	$1.3389466(3) \times 10^{-2}$	$1.3389465(7) \times 10^{-2}$	3×10^{-8}

(8) The gauge fields are then constructed as discussed at the end of Sec. IV B following the hierarchical structure given in Table I.

(9) The metric and its derivatives are constructed using the formulas given in Appendix A 6. The self-force is then constructed via Eq. (3.1).

For comparison we also compute the retarded field with the method described in Sec. II C. The first four steps of the algorithm in this case are the same as those above. Then for the fifth step we use Eq. (2.22) to construct the retarded-field weighting coefficients. This step only requires
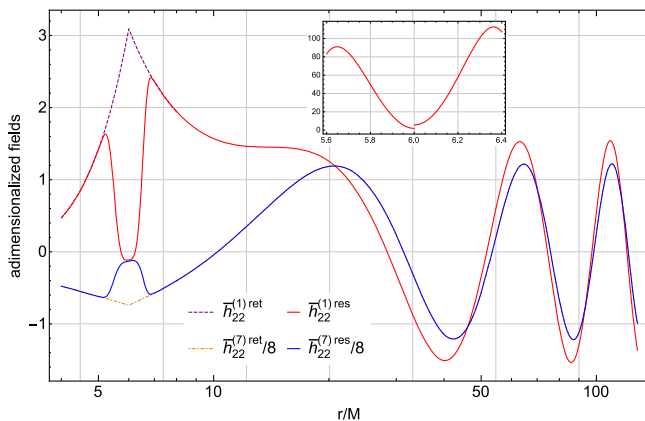

FIG. 2 (color online).   Sample results for the $\ell = 2$, $m = 2$ mode for a particle orbiting at $r_0 = 6M$. Shown are the $\bar{h}^{(1)}$ and (scaled) $\bar{h}^{(7)}$ metric perturbations for both the residual and retarded fields. At $r = 6M$, the upper solid (red) curve shows the residual field $\bar{h}^{(1)\text{res}}$. The dashed (purple) curve shows the retarded field $\bar{h}^{(1)\text{ret}}$. Far from the particle the two coincide. Similarly, the lower solid (blue) curve shows $\bar{h}^{(7)\text{res}}$ and the dot-dashed (orange) curve shows $\bar{h}^{(7)\text{ret}}$. The inset shows $\bar{h}_{,rr}^{(1)\text{res}}$ near the particle. With the punctures we present in the main text the residual fields are C^1 at the particle and correspondingly, as the inset shows, the second radial derivatives of the residual field are discontinuous. As the residual fields are C^1 at the particle the self-force can be directly computed from their derivatives. The punctures we provide online in Supplemental Material [57] give C^2 residual fields at the particle which acts to improve the convergence rate of the mode sum, as shown in Fig. 3.

knowledge of the homogeneous fields and the sources given in Appendix B. The retarded solutions are then constructed using Eq. (2.21). Finally we compute the self-force with both the standard mode-sum prescription described in Sec. III A (which relies on projecting the retarded tensor modes onto a basis of spherical-harmonics before regularization) and the tensor mode-sum prescription we present in Sec. VI. Note that only the radial component of the self-force requires regularization as it is the only component with nonzero regularization parameters [see Eq. (3.12)]. Correspondingly, the contributions to both the t and φ components of the self-force converge exponentially in both $\hat{\ell}$ and ℓ (the θ component is zero by symmetry).

C. Results

Using the above algorithm we can compute the residual metric perturbation at $r = r_0$. Using the residual field at the particle we can compute h_{uu}^R and we find that our results agree with previously published results to a relative accuracy of 10^{-7}. Taking a radial derivative of the residual metric perturbation at the particle, we can compute the radial self-force without any further regularization required. For the radial self-force we find agreement with the previous published results to a relative accuracy of 10^{-6}; see Table III. In Fig. 2 we plot the residual field for the $(\ell, m, i) = (2, 2, 1)$ field for a particle orbiting at $r_0 = 6M$.

A key feature of our procedure is that we only ever work with tensor-harmonic modes in constructing the self-force. This is in contrast to the standard mode-sum scheme whereby the tensor-harmonics of the retarded field are projected onto a basis of scalar harmonics before regularization. This projection, though straightforward, is cumbersome to implement (see, e.g., Appendix C in Ref. [33]). Furthermore the coupling between the tensor and scalar modes means that in practice to calculate $\hat{\ell}_{max}$ scalar modes one needs to calculate $\ell_{max} = \hat{\ell}_{max} + 3$ tensor modes. With our prescription this is not necessary.

In Fig. 3 we show the convergence of the tensor mode sum for the regular contributions to h_{uu}^R and F^r. The punctures we use in this work are sufficiently regular that,
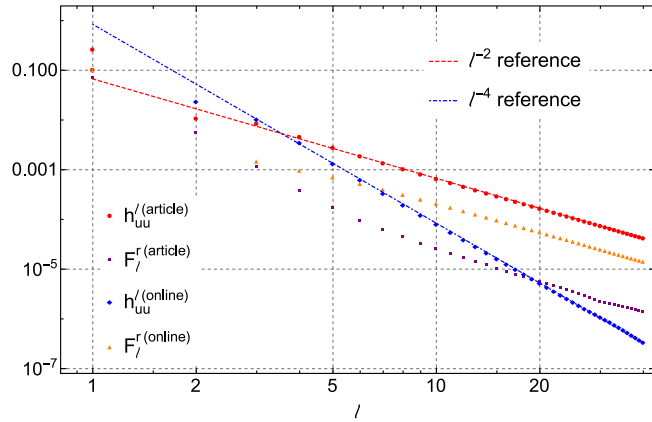
FIG. 3 (color online). Convergence of the *tensor* ℓ-mode contributions to (the adimensionalized) h_{uu} and F^r for a particle orbiting at $r_0 = 6M$. The punctures we present in this article in Appendix C are sufficiently regular that the contributions to h_{uu} and F^r drop off as ℓ^{-2}. Online we give higher-order punctures in Supplemental Material [57] that improve the rate of convergence for h_{uu} to ℓ^{-4}. This is not the case for F^r; the higher-order punctures are still one order lower than would be required to improve its rate of convergence. Instead, they merely change the coefficient of the ℓ^{-2} behavior in such a way that the infinite sum over ℓ is unaffected.

for high ℓ the contributions to h_{uu}^R and F^r drop off as ℓ^{-4} and ℓ^{-2}, respectively.

In the next section we show how, by taking the limit to the worldline in our effective-source procedure, we can formulate a tensor-mode mode-sum scheme.

VI. MODE-SUM REGULARIZATION WITH TENSOR-HARMONIC MODES

In addition to their use in the effective-source approach described here, the puncture fields may also be used to improve the efficiency of the traditional mode-sum scheme. In the standard mode-sum prescription, regularization is achieved through mode-sum formulas such as Eqs. (3.10) and (3.11), which take the form

$$F_\mu^R = \sum_{\hat{\ell}=0}^{\infty} [F_\mu^{\hat{\ell}\,\mathrm{ret}} - (2\hat{\ell}+1)F_\mu^{[-1]} - F_\mu^{[0]}] + D_\mu \qquad (6.1)$$

in the case of the self-force where we recall that an $\hat{\ell}$ sub-/superscript denotes the scalar-harmonic multipole contribution (summed over m). The regularization parameters $F_\mu^{[-1]}$ and $F_\mu^{[0]}$ are analytically derived functions of the instantaneous worldline. Provided the Detweiler-Whiting singular field is used in their derivation (and the retarded-field modes $F_\mu^{\hat{\ell}\,\mathrm{ret}}$ are in Lorenz gauge), the D_μ term vanishes. Each term in the sum goes like $\hat{\ell}^{-2}$ and so the partial sums converge as $\ell_{\max}^{-1}$. One can derive additional higher-order regularization parameters to accelerate this rate of convergence. For example, by subtracting an

appropriate term of the form $\frac{F_\mu^{[2]}}{(2\hat{\ell}-1)(2\hat{\ell}+3)}$ one finds that the terms in the sum now fall off as $\hat{\ell}^{-4}$. One can continue in this way to higher orders, where the order $\hat{\ell}^{-n}$ term has the form

$$\sum_{\hat{\ell}=0}^{\infty} \frac{2\hat{\ell}+1}{(2\hat{\ell}-n+1)(2\hat{\ell}-n+3)\ldots(2\hat{\ell}+n-1)(2\hat{\ell}+n+1)} = 0 \qquad (6.2)$$

for n even. The fact that the infinite sum over $\hat{\ell}$ vanishes is important as it guarantees that the subtraction of higher-order regularization parameters does not affect the numerical result (other than accelerating the rate of convergence); equivalently, these higher-order terms can be seen to come from pieces of the Detweiler-Whiting singular field which vanish when evaluated on the worldline.

In the scalar-field case, this mode-sum formula is a natural choice as one can choose to work with *scalar* spherical harmonics labeled by $\hat{\ell}$ when solving the field equations. In the gravitational case, the *tensor* spherical harmonics are a more natural choice and a numerical calculation typically produces tensor harmonic modes (labeled by ℓ) for the retarded field. Despite this fact, existing calculations have relied on a scalar-harmonic mode-sum formula of the form given in Eq. (6.1). As a result, a necessary step in the regularization procedure is the projection of the tensor-harmonic modes $F_\mu^{\ell\,\mathrm{ret}}$ onto scalar harmonic modes $F_\mu^{\hat{\ell}\,\mathrm{ret}}$. This is undesirable for at least two reasons: (i) the projection involves cumbersome mode coupling formulas which have to be derived on a case-by-case basis, and (ii) a given scalar-harmonic mode $\hat{\ell}$ couples to several tensor-harmonic modes (up to $\hat{\ell} \pm 2$ for the metric and higher for some of its derivatives). This second point means that in order to obtain a given number of scalar $\hat{\ell}$ modes, one actually has to compute several higher tensor-harmonic ℓ modes of the retarded field, and these are then lost during the projection. Given that the cost of computing a given retarded-field mode grows quadratically with ℓ, this turns out to be quite a significant increase in computational cost.

Fortunately, it turns out that the projection onto scalar harmonics is unnecessary; in this section we will derive tensor-harmonic regularization parameters which completely eliminate the need for scalar harmonics. This addresses both issues mentioned above and produces a much simpler, more accurate, and computationally efficient result.

First, we consider what form a tensor-harmonic mode-sum scheme should take. The ℓ dependence of the term of order ℓ^{-n} will be given by

$$\Lambda_{m,n} \equiv \frac{2^{n-2m}(2\ell+1)(\ell-m+1)_{2m}}{(2\ell-2m+n+1)(\ell-m+\frac{n}{2}+\frac{3}{2})_{2m-n}} \qquad (6.3)$$

for $m \geq 0$ and n integers. Here, we use the standard notation $(a)_n = a(a+1)\ldots(a+n-1)$ for the Pochhammer symbol. When $m = 0$ we can see that this reduces to the scalar-harmonic case (6.2), as expected. For $m > 0$ and $n \geq 2$ the infinite sum over ℓ of any of these terms is zero, meaning we are free to add them without modifying the final result (other than accelerating convergence). In Eq. (6.2) this was only true when the sum starts at $\ell = 0$, which would not be appropriate for tensor harmonics. For our generalized expression (6.3), this holds for the sum starting at any value in the range $0 \leq \ell \leq m$. In practice we will have m equal to the value of m' used in the punctures and n will be determined by the power of ρ appearing in the singular field.

Examining the puncture fields in Appendix C, we can see they are already written in a form where this ℓ dependence is manifestly apparent. The task of producing tensor-harmonic regularization parameters is therefore merely a matter of reconstructing the ℓ modes of the singular metric perturbation using the expressions given in Appendix A 6, summing over m and then evaluating on the worldline. It is most convenient to do so in the (α, β) coordinate system, i.e., using the punctures without the Wigner-D rotation matrices and evaluating at $\alpha = 0$, as then only a small number of m' modes must be summed over. The only caveat is that this yields the components of the metric in the (α, β) coordinates. We must therefore also include a factor of the Jacobian from (α, β) to (θ, φ) coordinates. This Jacobian is given by

$$\frac{\partial \alpha}{\partial \theta} = \frac{-\cos \alpha \sin \beta}{\sqrt{1 - \sin^2 \alpha \sin^2 \beta}} \approx 0, \qquad (6.4a)$$

$$\frac{\partial \alpha}{\partial \varphi} = \cos \beta \approx 1, \qquad (6.4b)$$

$$\frac{\partial \beta}{\partial \theta} = \frac{-\cos \beta}{\sin \alpha \sqrt{1 - \sin^2 \alpha \sin^2 \beta}} \approx -\frac{1}{\sin \alpha}, \qquad (6.4c)$$

$$\frac{\partial \beta}{\partial \phi} = \frac{-\cos \alpha \sin \beta}{\sin \alpha} \approx 0. \qquad (6.4d)$$

Note that because of the factor of $\frac{1}{\sin \alpha}$ appearing here, it is important to multiply by the Jacobian before taking the limit $\alpha \to 0$.

Since we are interested in computing the metric perturbation and its derivative (for the self-force), we require mode-sum formulas for all components of the metric perturbation and its derivative, i.e.,

$$h_{\mu\nu}^{\text{R}} = \sum_{\ell=0}^{\infty} [h_{\mu\nu}^{\ell \text{ret}} - h_{\mu\nu}^{[0]}] \qquad (6.5)$$

and

$$h_{\mu\nu,\gamma}^{\text{R}} = \sum_{\ell=0}^{\infty} [h_{\mu\nu,\gamma}^{\ell \text{ret}} - (2\ell+1)h_{\mu\nu,\gamma}^{[-1]} - h_{\mu\nu,\gamma}^{[0]}]. \qquad (6.6)$$

Here, the retarded-field ℓ modes are computed in the usual way from numerical data in the (θ, φ) coordinates,

$$h_{\mu\nu}^{\ell \text{ret}} \equiv \sum_{m=-\ell}^{\ell} h_{\mu\nu}^{\ell m}\left(r_0, \frac{\pi}{2}, 0\right), \qquad (6.7)$$

where the $h_{\mu\nu}^{\ell m}$ are constructed by combining the $h_{\ell m}^{(i)}$ with the spherical harmonics; explicit expressions are given in Appendix A 6. The regularization parameters for the metric perturbation are computed using

$$h_{\mu\nu}^{[0]} = \sum_{m'=-\ell}^{\ell} \left[\frac{\partial x^{\mu'}}{\partial x^\mu}\frac{\partial x^{\nu'}}{\partial x^\nu} h_{\mu'\nu'}^{P\ell m'}\right]_{x=x_0}, \qquad (6.8)$$

where x_0 denotes the point on the worldline, i.e., $r = r_0$ and $\alpha = 0 = \beta$. The only nonzero contributions in our case come from $m' = 0$ in the scalar sector ($i = 1, 3, 6$), $m' = \pm 1$ in the vector sector ($i = 4, 8$), and $m' = \pm 2$ in the tensor sector ($i = 7, 10$). The regularization parameters for the radial derivative of the metric perturbation are computed using

$$h_{\mu\nu,r}^{[0]} = \sum_{m'=-\ell}^{\ell} \left[\frac{\partial x^{\mu'}}{\partial x^\mu}\frac{\partial x^{\nu'}}{\partial x^\nu} \partial_r h_{\mu'\nu'}^{P\ell m'}\right]_{x=x_0}, \qquad (6.9)$$

where again the only nonzero contributions in this case come from $m' = 0$ in the scalar sector ($i = 1, 3, 6$), $m' = \pm 1$ in the vector sector ($i = 4, 8$), and $m' = \pm 2$ in the tensor sector ($i = 7, 10$). Finally, the regularization parameters for the φ derivative of the metric perturbation are computed using

$$h_{\mu\nu,\varphi}^{[0]} = \sum_{m'=-\ell}^{\ell} \left[\frac{\partial \alpha}{\partial \varphi}\partial_\alpha\left(\frac{\partial x^{\mu'}}{\partial x^\mu}\frac{\partial x^{\nu'}}{\partial x^\nu} h_{\mu'\nu'}^{P\ell m'}\right)\right]_{x=x_0}, \qquad (6.10)$$

where the only nonzero contributions in this case come from $m' = \pm 1$ for $h_{tr}^{P\ell m'}$ (i.e., $i = 2$) and $m' = (0, \pm 2)$ for $h_{rA}^{P\ell m'}$ (i.e., $i = 5, 9$). Evaluating these with the punctures given in Appendix C yields the following tensor-harmonic regularization parameters:

$$h_{tt}^{[0]} = \frac{4(r_0 - M)\mathcal{K}}{\pi r_0^2}\sqrt{\frac{r_0 - 2M}{r_0 - 3M}}, \qquad (6.11a)$$

$$h_{t\varphi}^{[0]} = -\frac{32M^{1/2}\mathcal{K}}{\pi r_0^{1/2}}\sqrt{\frac{r_0 - 2M}{r_0 - 3M}}\Lambda_1, \qquad (6.11b)$$

$$h_{rr}^{[0]} = \frac{4\mathcal{K}}{\pi}\frac{(r_0 - 3M)^{1/2}}{(r_0 - 2M)^{3/2}}, \qquad (6.11c)$$

$$h_{\theta\theta}^{[0]} = \frac{4r_0\mathcal{K}}{\pi}\sqrt{\frac{r_0 - 2M}{r_0 - 3M}} - \frac{64Mr_0\mathcal{K}}{\pi(r_0 - 2M)^{1/2}(r_0 - 3M)^{1/2}}\Lambda_2,$$

(6.11d)

$$h_{\varphi\varphi}^{[0]} = \frac{4r_0\mathcal{K}}{\pi}\sqrt{\frac{r_0 - 2M}{r_0 - 3M}} + \frac{64Mr_0\mathcal{K}}{\pi(r_0 - 2M)^{1/2}(r_0 - 3M)^{1/2}}\Lambda_2,$$

(6.11e)

$$h_{tt,r}^{[-1]} = \mp\frac{(r_0 - M)}{r_0^{5/2}(r_0 - 3M)^{1/2}},$$

(6.11f)

$$h_{tt,r}^{[0]} = \frac{2(r_0 - M)[(r_0 - 2M)\mathcal{E} - 2(r_0 - 4M)\mathcal{K}]}{\pi r_0^3(r_0 - 3M)^{1/2}(r_0 - 2M)^{1/2}},$$

(6.11g)

$$h_{rr,r}^{[-1]} = \mp\frac{(r_0 - 3M)^{1/2}}{r_0^{1/2}(r_0 - 2M)^2},$$

(6.11h)

$$h_{rr,r}^{[0]} = \frac{2(r_0 - 3M)^{1/2}[(r_0 - 2M)\mathcal{E} - 2r_0\mathcal{K}]}{\pi r_0(r_0 - 2M)^{5/2}},$$

(6.11i)

$$h_{t\varphi,r}^{[-1]} = \pm\left[\frac{2M^{1/2}}{r_0(r_0 - 3M)^{1/2}}\right]_{\ell\geq1},$$

(6.11j)

$$h_{t\varphi,r}^{[0]} = -\frac{16M^{1/2}[(r_0 - 2M)\mathcal{E} + 2M\mathcal{K}]}{\pi r_0^{3/2}(r_0 - 3M)^{1/2}(r_0 - 2M)^{1/2}}\Lambda_1,$$

(6.11k)

$$h_{\varphi\varphi,r}^{[-1]} = \mp\sqrt{\frac{r_0}{r_0 - 3M}}\mp\left[\frac{Mr_0^{1/2}}{(r_0 - 2M)(r_0 - 3M)^{1/2}}\right]_{\ell\geq2},$$

(6.11l)

$$h_{\varphi\varphi,r}^{[0]} = \frac{2(\mathcal{E} + 2\mathcal{K})}{\pi}\sqrt{\frac{r_0 - 2M}{r_0 - 3M}}$$
$$+ \frac{32M(\mathcal{E} + 2\mathcal{K})}{\pi(r_0 - 3M)^{1/2}(r_0 - 2M)^{1/2}}\Lambda_2,$$

(6.11m)

$$h_{\theta\theta,r}^{[-1]} = \mp\sqrt{\frac{r_0}{r_0 - 3M}}\pm\left[\frac{Mr_0^{1/2}}{(r_0 - 2M)(r_0 - 3M)^{1/2}}\right]_{\ell\geq2},$$

(6.11n)

$$h_{\theta\theta,r}^{[0]} = \frac{2(\mathcal{E} + 2\mathcal{K})}{\pi}\sqrt{\frac{r_0 - 2M}{r_0 - 3M}}$$
$$- \frac{32M(\mathcal{E} + 2\mathcal{K})}{\pi(r_0 - 3M)^{1/2}(r_0 - 2M)^{1/2}}\Lambda_2,$$

(6.11o)

$$h_{tr,\varphi}^{[0]} = -\frac{32((r_0 - 2M)\mathcal{E} - (r_0 - 3M)\mathcal{K})}{\pi M^{1/2}r_0^{3/2}}\sqrt{\frac{r_0 - 2M}{r_0 - 3M}}\Lambda_1,$$

(6.11p)

$$h_{r\varphi,\varphi}^{[0]} = \frac{16[(r_0 - 2M)\mathcal{E} - (r_0 - 3M)\mathcal{K}]}{\pi(r_0 - 2M)^{1/2}(r_0 - 3M)^{1/2}}(\Lambda_1 + 4\Lambda_2),$$

(6.11q)

where we recall that Λ_1 and Λ_2 are given by Eqs. (4.9) and (4.10), respectively, and where we have indicated with a subscript the cases ($h_{t\varphi,r}^{[-1]}$, $h_{\theta\theta,r}^{[-1]}$, and $h_{\varphi\varphi,r}^{[-1]}$) where a term is only nonzero above some minimum value of ℓ. In all of the above equations, to simplify the presentation we have omitted an overall factor of the small mass μ.

Finally, we note that these expressions can be combined to produce tensor-harmonic regularization parameters for the redshift invariant $h_{\mu\nu}u^\mu u^\nu$ and the radial component of the self-force. Doing so, we find

$$H^{[0]} = \frac{4\mu}{\pi\sqrt{r_0^2 + L_0^2}}\mathcal{K}$$
$$- \frac{1}{(2\ell - 1)(2\ell + 3)}\frac{8\mu M(6r_0 - 17M)\mathcal{K}}{\pi r_0(r_0 - 3M)^{3/2}(r_0 - 2M)^{1/2}}$$
$$+ \frac{1}{(2\ell - 3)(2\ell - 1)(2\ell + 3)(2\ell + 5)}$$
$$\times\frac{420\mu M^2\mathcal{K}}{\pi r_0(r_0 - 3M)^{3/2}(r_0 - 2M)^{1/2}},$$

(6.12)

$$F_{[-1]}^{r\pm} = \mp\frac{\mu^2}{2r_0^2}\left(1 - \frac{3M}{r_0}\right)^{1/2}\pm\left[\frac{2\mu^2 M(2M - r_0)}{r_0^{5/2}(r_0 - 3M)^{3/2}}\right]_{\ell<1}$$
$$\pm\left[\frac{\mu^2 M^2}{2r_0^{5/2}(r_0 - 3M)^{3/2}}\right]_{\ell<2},$$

(6.13)

$$F_{[0]}^r = \frac{\mu^2 r_0 E_0^2}{\pi(L_0^2 + r_0^2)^{3/2}}[\mathcal{E} - 2\mathcal{K}] - \frac{1}{(2\ell - 1)(2\ell + 3)}$$
$$\times\frac{2\mu^2 M(r_0 - 2M)^{1/2}[(6r_0 - 17M)\mathcal{E} + 2M\mathcal{K}]}{\pi r_0^3(r_0 - 3M)^{3/2}}$$
$$+ \frac{1}{(2\ell - 3)(2\ell - 1)(2\ell + 3)(2\ell + 5)}$$
$$\times\frac{105\mu^2 M^2(r_0 - 2M)^{1/2}(\mathcal{E} + 2\mathcal{K})}{\pi r_0^3(r_0 - 3M)^{3/2}}.$$

(6.14)

Note that in giving these parameters we have rewritten Λ_1 and Λ_2 in a form which highlights the fact that $H^{[0]}$ and $F_{[0]}^r$ both match their scalar-harmonic counterparts [Eq. (3.12)], with the exception of higher-order terms in $1/\ell$. Since these terms vanish when summed from $\ell = 0$ to infinity they have no impact on the final result and can be ignored in

practice. Importantly, this is not the case for $F^{r\pm}_{[-1]}$ which differs from its scalar-harmonic version. The difference is in the presence of the second and third terms, which arises from the fact our mode sum expression (6.9) starts at $\ell = 0$ while it should start at $\ell = 1$ for the vector sector and at $\ell = 2$ for the tensor sector. However, since this term has different limits on either side of the worldline, it vanishes upon averaging the left and right radial limits. As such, we see that in this case regularization can be achieved without projection onto scalar harmonics by using the scalar-harmonic regularization parameters combined with an averaging procedure.

VII. CONCLUDING REMARKS

In this work we have developed a frequency-domain application of the effective source approach to computing the self-force on a point mass in a curved background spacetime. This new method builds on previous work which studied the case of a scalar-field toy model [28], extending it to the more physically relevant gravitational case.

With a numerical implementation for the case of a circular orbit in Schwarzschild spacetime, our results demonstrate that the method can reliably produce accurate numerical results for the regularized metric perturbation with modest effort and computational cost. While this is not particularly important in a first-order calculation—the traditional mode-sum method, for example, can already produce comparable results with similar or better computational efficiency—the primary goal of our approach is to develop a set of methods which will be applicable to a second-order self-force calculation. Our results provide two key components in that regard.

(1) Our numerical scheme for solving the sourced field equations in the frequency domain carries over immediately to second order. The only change will be that the source will be a more complicated function involving the first-order metric perturbation.

(2) The source for the second-order field equations is most efficiently written in terms of the first-order Detweiler-Whiting regular field in an extended region near the worldline. Such an approximation is exactly the output from our first-order calculation.

In addition to addressing several important aspects of a second-order self-force calculation, the tensor-harmonic regularization parameters we derived in Sec. VI can also be used to improve the computational efficiency of a first-order mode-sum self-force calculation by avoiding the need for a cumbersome and wasteful projection onto scalar harmonics. It is interesting to note the close relation between the tensor-harmonic regularization parameters and those one would obtain using a scalar-harmonic decomposition. In particular, provided one computes an average of either side of the (radial) limit to the worldline, we have found that scalar-harmonic regularization parameters may be used in place of their tensor-harmonic counterparts. We anticipate that this is more than merely a coincidence; in a future work we will investigate whether a similar result holds in more general cases.

There are several future directions in which our results may be extended. Most important is the application of our approach to the calculation of conservative effects from the second-order gravitational self-force [9,24,25]. In addition to this, it may be interesting to study extensions of the approach beyond circular orbits, to the Kerr spacetime and to radiation and Regge-Wheeler gauges. With a view to identifying other important second-order effects, it may also be interesting to incorporate our method into an orbital evolution scheme which makes use of a two-timescale expansion of the equations of motion [58]. Such a scheme would likely provide a compelling balance of computational efficiency and faithfulness to the underlying physics of extreme-mass-ratio inspirals.

APPENDIX A: FUNCTIONS ON THE TWO-SPHERE

When dealing with functions on the two-sphere, there are a wide number of possible conventions. Our conventions, which are consistent with those of MATHEMATICA [59], are summarized in this appendix.

1. Scalar spherical harmonics

The associated Legendre polynomials may be defined in terms of derivatives of the standard Legendre polynomials,

$$P^m_\ell(x) = (-1)^m (1-x^2)^{m/2} \frac{d^m}{dx^m} P_\ell(x) \quad [m \geq 0], \qquad \text{(A1a)}$$

$$P^{-m}_\ell(x) = (-1)^m \frac{(\ell-m)!}{(\ell+m)!} P^m_\ell(x), \qquad \text{(A1b)}$$

where we have included the Condon-Shortley phase factor $(-1)^m$ and where the Legendre polynomials satisfy the Legendre equation

$$(1 - x^2)\frac{d^2 P_\ell(x)}{dx^2} - 2x\frac{dP_\ell(x)}{dx} + \ell(\ell+1)P_\ell(x) = 0.$$

(A2)

We now define the scalar spherical harmonics as

$$Y_{\ell m}(\theta, \varphi) = \sqrt{\frac{(2\ell+1)}{4\pi}\frac{(\ell-m)!}{(\ell+m)!}}P_\ell^m(\cos\theta)e^{im\varphi},$$

(A3)

where $-\ell \leq m \leq \ell$. Note that ℓ and m are merely labels and we will raise and lower their position freely to wherever they get in the way the least. The scalar spherical harmonics are orthonormal,

$$\int_0^{2\pi}\int_0^\pi Y_{\ell m}(\theta, \varphi)Y^*_{\ell' m'}(\theta, \varphi)d\Omega = \delta_{\ell\ell'}\delta_{mm'},$$

(A4)

where $d\Omega \equiv \sin\theta d\theta d\varphi$. They also satisfy

$$Y^*_{\ell m}(\theta, \varphi) = (-1)^m Y_{\ell, -m}(\theta, \varphi),$$

(A5)

and the completeness relation

$$\sum_{\ell=0}^\infty \sum_{m=-\ell}^\ell Y_{\ell m}(\theta, \varphi)Y^*_{\ell m}(\theta', \varphi') = \delta(\cos\theta - \cos\theta')\delta(\varphi - \varphi').$$

(A6)

Since the scalar harmonics form an orthonormal basis, an arbitrary scalar function can be expanded in spherical harmonics,

$$f(\theta, \varphi) = \sum_{\ell=0}^\infty \sum_{m=-\ell}^\ell f_{\ell m}Y_{\ell m}(\theta, \varphi),$$

(A7)

where the coefficients are given by

$$f_{\ell m} = \int_0^{2\pi}\int_0^\pi f(\theta, \varphi)Y^*_{\ell m}(\theta, \varphi)d\Omega.$$

(A8)

At the pole, $\theta = 0$, only the $m = 0$ spherical harmonics are nonzero, and Eq. (A7) becomes

$$f(0, \varphi) = \sum_{\ell=0}^\infty \sqrt{\frac{2\ell+1}{4\pi}}f_{\ell 0},$$

(A9)

where

$$f_{\ell 0} = \sqrt{\frac{2\ell+1}{4\pi}}\int_0^{2\pi}\int_0^\pi f(\alpha, \beta)P_\ell(\cos\alpha)d\Omega.$$

(A10)

Similarly, the θ derivative only requires modes $m = -1, 1$,

$$(\partial_\theta f)(0, \varphi) = \sum_{\ell=0}^\infty \sqrt{\frac{\ell(\ell+1)(2\ell+1)}{16\pi}}(e^{-i\varphi}f_{\ell, -1} - e^{i\varphi}f_{\ell 1}),$$

(A11)

the second θ derivative requires $m = 0, \pm 2$,

$$(\partial_{\theta\theta}f)(0, \varphi) = \sum_{\ell=0}^\infty \sqrt{\frac{(2\ell+1)}{64\pi}}\Big[-2\ell(\ell+1)f_{\ell 0}$$
$$+ \sqrt{(\ell-1)\ell(\ell+1)(\ell+1)}$$
$$\times (e^{-2i\beta}f_{\ell, -2} + e^{2i\beta}f_{\ell 2})\Big],$$

(A12)

and so on; for n derivatives with respect to θ we need modes $m = -n, -n+2, \ldots, n-2, n$.

2. Vector spherical harmonics

The vector spherical harmonics fall into two categories: those of even parity ($\ell + m$ even) and those of odd parity ($\ell + m$ odd). These categories reflect a difference in behavior under the parity operation $(\theta, \varphi) \to (\pi - \theta, \varphi + \pi)$; the even-parity harmonics are invariant under this transformation while the odd-parity harmonics change sign.

The even-parity vector harmonics are defined by

$$Z_A^{\ell m} = [\ell(\ell+1)]^{-1/2}D_A Y^{\ell m},$$

(A13)

and the odd-parity harmonics are defined by

$$X_A^{\ell m} = -[\ell(\ell+1)]^{-1/2}\epsilon_A{}^B D_B Y^{\ell m},$$

(A14)

where D_A is the covariant derivative and ϵ_{AB} is the Levi-Civita tensor associated with the metric $\Omega_{AB} = \mathrm{diag}(1, \sin^2\theta)$ on the two-sphere (i.e., $\epsilon_{\theta\varphi} = \sin\theta$, $\epsilon_{\varphi\theta} = -\sin\theta$, $\epsilon_{\theta\theta} = 0 = \epsilon_{\varphi\varphi}$). Explicitly, the components of the vector harmonics are

$$Z_\theta^{\ell m} = [\ell(\ell+1)]^{-1/2}\partial_\theta Y^{\ell m},$$
$$X_\theta^{\ell m} = -[\ell(\ell+1)]^{-1/2}\frac{1}{\sin\theta}\partial_\varphi Y^{\ell m},$$
$$Z_\varphi^{\ell m} = [\ell(\ell+1)]^{-1/2}\partial_\varphi Y^{\ell m},$$
$$X_\varphi^{\ell m} = [\ell(\ell+1)]^{-1/2}\sin\theta\,\partial_\theta Y^{\ell m}.$$

(A15)

The vector harmonics satisfy the orthonormality relations

$$\int_0^{2\pi}\int_0^\pi X_A^{\ell m}(\theta, \varphi)X_{\ell' m'}^{A*}(\theta, \varphi)d\Omega = \delta_{\ell\ell'}\delta_{mm'},$$

(A16a)

$$\int_0^{2\pi}\int_0^\pi Z_A^{\ell m}(\theta, \varphi)Z_{\ell' m'}^{A*}(\theta, \varphi)d\Omega = \delta_{\ell\ell'}\delta_{mm'},$$

(A16b)

$$\int_0^{2\pi}\int_0^\pi X_A^{\ell m}(\theta, \varphi)Z_{\ell' m'}^{A*}(\theta, \varphi)d\Omega = 0.$$

(A16c)

They also satisfy

$$X_A^{\ell m*}(\theta, \varphi) = (-1)^m X_A^{\ell, -m}(\theta, \varphi),$$

(A17a)

$$Z_A^{\ell m*}(\theta, \varphi) = (-1)^m Z_A^{\ell, -m}(\theta, \varphi). \qquad \text{(A17b)}$$

These definitions are consistent with Ref. [60] and with Ref. [61] [apart from the inclusion of the prefactor $[\ell(\ell+1)]^{-1/2}$ which ensures orthonormality] and relate to those of Ref. [62] through the conversion $Z_A^{\ell m} \to [\ell(\ell+1)]^{1/2} Y_A^{\ell m}$, $X_A^{\ell m} \to [\ell(\ell+1)]^{1/2} X_A^{\ell m}$.

3. Tensor spherical harmonics

The tensor spherical harmonics again fall into two categories: those of even parity ($\ell + m$ even) and those of odd parity ($\ell + m$ odd). The even-parity tensor harmonics are defined by

$$Z_{AB}^{\ell m} = \left[2\frac{(\ell-2)!}{(\ell+2)!}\right]^{\frac{1}{2}}\left[D_A D_B + \frac{1}{2}\ell(\ell+1)\Omega_{AB}\right]Y^{\ell m},$$
$$\text{(A18)}$$

and the odd-parity harmonics are defined by

$$X_{AB}^{\ell m} = -\left[2\frac{(\ell-2)!}{(\ell+2)!}\right]^{\frac{1}{2}}\epsilon_{(A}{}^C D_{B)} D_C Y^{\ell m}. \qquad \text{(A19)}$$

Explicitly, the components of the tensor harmonics are

$$Z_{\theta\theta}^{\ell m} = \left[2\frac{(\ell-2)!}{(\ell+2)!}\right]^{\frac{1}{2}}\left[\partial_{\theta\theta} + \frac{1}{2}\ell(\ell+1)\right]Y^{\ell m}, \qquad \text{(A20a)}$$

$$Z_{\theta\varphi}^{\ell m} = \left[2\frac{(\ell-2)!}{(\ell+2)!}\right]^{\frac{1}{2}}[\partial_{\theta\varphi} - \cot\theta\,\partial_\varphi]Y^{\ell m}, \qquad \text{(A20b)}$$

$$Z_{\varphi\varphi}^{\ell m} = \left[2\frac{(\ell-2)!}{(\ell+2)!}\right]^{\frac{1}{2}}[\partial_{\varphi\varphi} + \sin\theta\,\cos\theta\,\partial_\theta$$
$$+ \frac{1}{2}\ell(\ell+1)\sin^2\theta]Y^{\ell m}, \qquad \text{(A20c)}$$

$$X_{\theta\theta}^{\ell m} = -\left[2\frac{(\ell-2)!}{(\ell+2)!}\right]^{\frac{1}{2}}\frac{1}{\sin\theta}[\partial_{\theta\varphi} - \cot\theta\,\partial_\varphi]Y^{\ell m}, \qquad \text{(A20d)}$$

$$X_{\theta\varphi}^{\ell m} = -\left[2\frac{(\ell-2)!}{(\ell+2)!}\right]^{\frac{1}{2}}\frac{1}{2\sin\theta}[\partial_{\varphi\varphi} - \sin^2\theta\partial_{\theta\theta}$$
$$+ \sin\theta\,\cos\theta\,\partial_\theta]Y^{\ell m}, \qquad \text{(A20e)}$$

$$X_{\varphi\varphi}^{\ell m} = \left[2\frac{(\ell-2)!}{(\ell+2)!}\right]^{\frac{1}{2}}\sin\theta[\partial_{\theta\varphi} - \cot\theta\,\partial_\varphi]Y^{\ell m}. \qquad \text{(A20f)}$$

The tensor harmonics satisfy the orthonormality relations

$$\int_0^{2\pi}\int_0^\pi X_{AB}^{\ell m}(\theta, \varphi)X_{\ell'm'}^{AB*}(\theta, \varphi)d\Omega = \delta_{\ell\ell'}\delta_{mm'}, \qquad \text{(A21a)}$$

$$\int_0^{2\pi}\int_0^\pi Z_{AB}^{\ell m}(\theta, \varphi)Z_{\ell'm'}^{AB*}(\theta, \varphi)d\Omega = \delta_{\ell\ell'}\delta_{mm'}, \qquad \text{(A21b)}$$

$$\int_0^{2\pi}\int_0^\pi X_{AB}^{\ell m}(\theta, \varphi)Z_{\ell'm'}^{AB*}(\theta, \varphi)d\Omega = 0, \qquad \text{(A21c)}$$

and the identity

$$\Omega^{AB}Z_{AB}^{\ell m} = 0 = \Omega^{AB}X_{AB}^{\ell m}. \qquad \text{(A22)}$$

They also satisfy

$$X_{AB}^{\ell m*}(\theta, \varphi) = (-1)^m X_{AB}^{\ell, -m}(\theta, \varphi), \qquad \text{(A23a)}$$

$$Z_{AB}^{\ell m*}(\theta, \varphi) = (-1)^m Z_{AB}^{\ell, -m}(\theta, \varphi). \qquad \text{(A23b)}$$

These definitions are consistent with Thorne [60] and relate to those of Ref. [61] through an orthonormality factor, $Z_{AB}^{\ell m} \to [2\frac{(\ell-2)!}{(\ell+2)!}]^{1/2}Y_{AB}^{\ell m}$, $X_{AB}^{\ell m} \to [2\frac{(\ell-2)!}{(\ell+2)!}]^{1/2}X_{AB}^{\ell m}$.

4. Rotations

Under a rotation of the coordinate system which is represented by the Euler angles α, β, γ, the spherical harmonic components transform according to

$$f_{\ell m}(\theta, \varphi) = \sum_{m'=-\ell}^{\ell} D_{mm'}^{\ell}(\alpha, \beta, \gamma)f_{\ell m'}(\theta', \varphi'), \qquad \text{(A24)}$$

where $D_{mm'}^{\ell}(\alpha, \beta, \gamma)$ is the Wigner-D matrix [63]. Here, we use the convention that the Euler angles correspond to a $z - y - z$ counterclockwise rotation and our convention[3] for $D_{mm'}^{\ell}(\alpha, \beta, \gamma)$ is consistent with Rose [64]. Using these conventions, the Wigner-D matrix satisfies

$$D_{m_1 m_2}^{\ell}(\alpha, \beta, \gamma) = e^{-im_1\alpha - im_2\gamma}D_{m_1 m_2}^{\ell}(0, \beta, 0). \qquad \text{(A25)}$$

The vector and tensor harmonics also transform in a similar way [65], i.e.,

$$X_A^{\ell m}(\theta, \varphi) = \frac{\partial x^{A'}}{\partial x^A}\sum_{m'=-\ell}^{\ell} D_{mm'}^{\ell}(\alpha, \beta, \gamma)X_{A'}^{\ell m'}(\theta', \varphi'), \qquad \text{(A26a)}$$

$$Z_A^{\ell m}(\theta, \varphi) = \frac{\partial x^{A'}}{\partial x^A}\sum_{m'=-\ell}^{\ell} D_{mm'}^{\ell}(\alpha, \beta, \gamma)Z_{A'}^{\ell m'}(\theta', \varphi'), \qquad \text{(A26b)}$$

---

[3]This convention is different from that of MATHEMATICA [59] and Wigner [63]. Our $D_{mm'}^{\ell}(\alpha, \beta, \gamma)$ is related to theirs by a change in the signs of m and m' [64].

$$X_{AB}^{\ell m}(\theta,\varphi) = \frac{\partial x^{A'}}{\partial x^A}\frac{\partial x^{B'}}{\partial x^B}\sum_{m'=-\ell}^{\ell} D_{mm'}^\ell(\alpha,\beta,\gamma)X_{A'B'}^{\ell m'}(\theta',\varphi'),$$

(A26c)

$$Z_{AB}^{\ell m}(\theta,\varphi) = \frac{\partial x^{A'}}{\partial x^A}\frac{\partial x^{B'}}{\partial x^B}\sum_{m'=-\ell}^{\ell} D_{mm'}^\ell(\alpha,\beta,\gamma)Z_{A'B'}^{\ell m'}(\theta',\varphi'),$$

(A26d)

which is equivalent to stating that the vector- and tensor-harmonic components of a tensor transform according to Eq. (A24). Finally, we note that the Wigner-D matrix relates to the spin-weighted spherical harmonics,

$$D_{ms}^\ell(\alpha,\beta,\gamma) = (-1)^s\sqrt{\frac{4\pi}{2\ell+1}}\,_{-s}Y_{\ell m}^*(\beta,\alpha)e^{-is\gamma},$$

(A27)

which for the spin-0 case gives a relation to the scalar harmonics,

$$D_{m0}^\ell(\alpha,\beta,0) = \sqrt{\frac{4\pi}{2\ell+1}}Y_{\ell m}^*(\beta,\alpha).$$

(A28)

5. Tensor-harmonic basis in Schwarzschild spacetime

Barack and Lousto [39] used the above bases of scalar, vector, and tensor harmonics to construct a basis of harmonics for the components of a symmetric rank-2 tensor $t_{\mu\nu}$ defined on a Schwarzschild background spacetime. This basis was later modified slightly by Barack and Sago [33] to improve the behavior of some components near the horizon. In particular, they chose a basis of ten fields in $t-r$ space defined by

$$t_{\ell m}^{(1)} = \int_0^{2\pi}\int_0^\pi r(t_{tt}+f^2 t_{rr})Y_{\ell m}^*d\Omega,$$

(A29a)

$$t_{\ell m}^{(2)} = \int_0^{2\pi}\int_0^\pi 2rf t_{tr}Y_{\ell m}^*d\Omega,$$

(A29b)

$$t_{\ell m}^{(3)} = \int_0^{2\pi}\int_0^\pi rf^{-1}(t_{tt}-f^2 t_{rr})Y_{\ell m}^*d\Omega,$$

(A29c)

$$t_{\ell m}^{(4)} = \int_0^{2\pi}\int_0^\pi 2[\ell(\ell+1)]^{1/2}t_{tA}Z_{\ell m}^{A*}d\Omega,$$

(A29d)

$$t_{\ell m}^{(5)} = \int_0^{2\pi}\int_0^\pi 2[\ell(\ell+1)]^{1/2}f t_{rA}Z_{\ell m}^{A*}d\Omega,$$

(A29e)

$$t_{\ell m}^{(6)} = \int_0^{2\pi}\int_0^\pi \frac{1}{r}t_{AB}\Omega^{AB}Y_{\ell m}^*d\Omega,$$

$$t_{\ell m}^{(7)} = \int_0^{2\pi}\int_0^\pi \frac{1}{r}\left[2\frac{(\ell-2)!}{(\ell+2)!}\right]^{1/2}$$
$$\times t_{AB}\left(Z_{\ell m}^{AB*}-\frac{1}{2}\Omega^{AB}\Omega_{CD}Z_{\ell m}^{CD*}\right)d\Omega,$$

(A29f)

$$t_{\ell m}^{(8)} = -\int_0^{2\pi}\int_0^\pi 2[\ell(\ell+1)]^{1/2}t_{tA}X_{\ell m}^{A*}d\Omega,$$

(A29g)

$$t_{\ell m}^{(9)} = -\int_0^{2\pi}\int_0^\pi 2[\ell(\ell+1)]^{1/2}t_{rA}X_{\ell m}^{A*}d\Omega,$$

(A29h)

$$t_{\ell m}^{(10)} = \int_0^{2\pi}\int_0^\pi \frac{1}{r}\left[2\frac{(\ell-2)!}{(\ell+2)!}\right]^{1/2}$$
$$\times t_{AB}\left(X_{\ell m}^{AB*}-\frac{1}{2}\Omega^{AB}\Omega_{CD}X_{\ell m}^{CD*}\right)d\Omega,$$

(A29i)

where $f\equiv(1-2M/r)$. The harmonics $i=1,\dots,7$ are of even parity, while the harmonics $i=8,9,10$ are of odd parity.

Barack and Sago represented this basis in terms of a set of ten tensors defined by

$$Y_{\mu\nu}^{(1)} = \frac{1}{\sqrt{2}}(\delta_\mu^t\delta_\nu^t + f^{-2}\delta_\mu^r\delta_\nu^r)Y^{\ell m},$$

(A30)

$$Y_{\mu\nu}^{(2)} = \frac{1}{f\sqrt{2}}(\delta_\mu^t\delta_\nu^r + \delta_\mu^r\delta_\nu^t)Y^{\ell m},$$

(A31)

$$Y_{\mu\nu}^{(3)} = \frac{f}{\sqrt{2}}(\delta_\mu^t\delta_\nu^t - f^{-2}\delta_\mu^r\delta_\nu^r)Y^{\ell m},$$

(A32)

$$Y_{\mu\nu}^{(4)} = \frac{r}{\sqrt{2}}(\delta_\mu^t Z_\nu^{\ell m} + Z_\mu^{\ell m}\delta_\nu^t),$$

(A33)

$$Y_{\mu\nu}^{(5)} = \frac{r}{f\sqrt{2}}(\delta_\mu^r Z_\nu^{\ell m} + Z_\mu^{\ell m}\delta_\nu^r),$$

(A34)

$$Y_{\mu\nu}^{(6)} = \frac{r^2}{\sqrt{2}}\Omega_{AB}\delta_\mu^A\delta_\nu^B Y^{\ell m},$$

(A35)

$$Y_{\mu\nu}^{(7)} = r^2\left(Z_{\mu\nu}^{\ell m} - \frac{1}{2}Z^A_{\ A}\Omega_{\mu\nu}\right),$$

(A36)

$$Y_{\mu\nu}^{(8)} = -\frac{r}{\sqrt{2}}(\delta_\mu^t X_\nu^{\ell m} + X_\mu^{\ell m}\delta_\nu^t),$$

(A37)

$$Y_{\mu\nu}^{(9)} = -\frac{r}{f\sqrt{2}}(\delta_\mu^r X_\nu^{\ell m} + X_\mu^{\ell m}\delta_\nu^r),$$

(A38)

$$Y_{\mu\nu}^{(10)} = r^2\left(X_{\mu\nu}^{\ell m} - \frac{1}{2}X^A_{\ A}\Omega_{\mu\nu}\right).$$

(A39)

With the exception of $i = 3$, this basis is an orthonormal set in the sense that

$$\int_0^{2\pi} \int_0^\pi \eta^{\tau\mu} \eta^{\kappa\nu} Y^{(i)\ell m}_{\mu\nu} Y^{(j)\ell'm'*}_{\tau\kappa} d\Omega = \delta_{ij}\delta_{\ell\ell'}\delta_{mm'}, \quad \text{(A40)}$$

where $\eta^{\tau\kappa} \equiv \text{diag}(1, f^2, r^{-2}, r^{-2}\sin^{-2}\theta)$. For $i = 3$, the set is also orthogonal, but $Y^{(3)}_{\mu\nu}$ has a norm of f^2.

Finally, we note that Barack and Sago factored out the coefficients

$$a^{(i)}_\ell = \frac{1}{\sqrt{2}} \begin{cases} 1, & i = 1,2,3,6, \\ (\ell(\ell+1))^{-1/2}, & i = 4,5,8,9, \\ ((\ell-1)\ell(\ell+1)(\ell+2))^{-1/2}, & i = 7,10 \end{cases}$$

(A41)

from the tensor-harmonic fields $\bar{h}^{(i)}$ in order to make some of their expressions for, e.g., the field equations more compact. We likewise use these coefficients in Eqs. (2.7) and (4.5).

6. Metric reconstruction

Rebuilding the original metric perturbation $h_{\mu\nu}$ from the $\bar{h}^{(i)}_{\ell m}$ fields is straightforward. The necessary equation can be derived using Eq. (A29) along with the fact that a trace reversal, $h_{\mu\nu} = \bar{h}_{\mu\nu} - \frac{1}{2}g_{\mu\nu}\bar{h}$, is equivalent to the interchange $h^{(3)} \Leftrightarrow h^{(6)}$. This gives

$$h_{\mu\nu} = \frac{\mu}{2r} \sum_\ell^\infty \sum_{m=-\ell}^\ell h^{\ell m}_{\mu\nu} e^{-i\omega_m t}, \quad \text{(A42)}$$

where

$$h^{\ell m}_{tt} = (\bar{h}^{(1)}_{\ell m} + f(r)\bar{h}^{(6)}_{\ell m})Y^{\ell m}, \quad \text{(A43)}$$

$$h^{\ell m}_{tr} = f(r)^{-1}\bar{h}^{(2)}_{\ell m}Y^{\ell m}, \quad \text{(A44)}$$

$$h^{\ell m}_{rr} = f(r)^{-2}(\bar{h}^{(1)}_{\ell m} - f\bar{h}^{(6)}_{\ell m})Y^{\ell m}, \quad \text{(A45)}$$

$$h^{\ell m}_{tA} = \frac{r}{\sqrt{\ell(\ell+1)}}(\bar{h}^{(4)}_{\ell m}Z^{\ell m}_A - \bar{h}^{(8)}_{\ell m}X^{\ell m}_A), \quad \text{(A46)}$$

$$h^{\ell m}_{rA} = \frac{r}{f(r)\sqrt{\ell(\ell+1)}}(\bar{h}^{(5)}_{\ell m}Z^{\ell m}_A - \bar{h}^{(9)}_{\ell m}X^{\ell m}_A), \quad \text{(A47)}$$

$$h^{\ell m}_{AB} = r^2\Omega_{AB}\bar{h}^{(3)}_{\ell m}Y^{\ell m}$$
$$+ r^2\sqrt{2\frac{(\ell-2)!}{(\ell+2)!}}\left(\bar{h}^{(7)}_{\ell m}\left(Z^{\ell m}_{AB} - \frac{1}{2}Z^C{}_C\Omega_{AB}\right)\right.$$
$$\left. - \bar{h}^{(10)}_{\ell m}\left(X^{\ell m}_{AB} - \frac{1}{2}X^C{}_C\Omega_{AB}\right)\right), \quad \text{(A48)}$$

and where the sum over ℓ begins at $\ell = 0$ for the scalar sector (i.e., $\bar{h}^1_{\ell m}, \bar{h}^2_{\ell m}, \bar{h}^3_{\ell m}$, and $\bar{h}^6_{\ell m}$), at $\ell = 1$ for the vector sector (i.e., $\bar{h}^4_{\ell m}, \bar{h}^5_{\ell m}, \bar{h}^8_{\ell m}$, and $\bar{h}^9_{\ell m}$), and at $\ell = 2$ for the tensor sector (i.e., $\bar{h}^7_{\ell m}$ and $\bar{h}^{10}_{\ell m}$).

APPENDIX B: FIELD EQUATIONS AND RETARDED FIELD SOURCES

The coupling terms in the frequency-domain field equation (2.10) are given by

$$\mathcal{M}^{(1)}{}_{(j)}\bar{h}^{(j)} = \frac{M}{r^2}f\bar{h}^{(3)}_{,r_*} + \frac{f}{2r^2}\left(1 - \frac{4M}{r}\right)(\bar{h}^{(1)} - \bar{h}^{(5)} - f\bar{h}^{(3)}) - \frac{f^2}{2r^2}\left(1 - \frac{6M}{r}\right)\bar{h}^{(6)}, \quad \text{(B1)}$$

$$\mathcal{M}^{(2)}{}_{(j)}\bar{h}^{(j)} = \frac{1}{2}ff'\bar{h}^{(3)}_{,r_*} + \frac{1}{2}f'[i\omega(\bar{h}^{(1)} - \bar{h}^{(2)}) + \bar{h}^{(2)}_{,r_*} - \bar{h}^{(1)}_{,r_*}] + \frac{f^2}{2r^2}(\bar{h}^{(2)} - \bar{h}^{(4)}) - \frac{ff'}{2r}(\bar{h}^{(1)} - \bar{h}^{(5)} - f\bar{h}^{(3)} - 2f\bar{h}^{(6)}), \quad \text{(B2)}$$

$$\mathcal{M}^{(3)}{}_{(j)}\bar{h}^{(j)} = -\frac{f}{2r^2}\left[\bar{h}^{(1)} - \bar{h}^{(5)} - \left(1 - \frac{4M}{r}\right)(\bar{h}^{(3)} + \bar{h}^{(6)})\right], \quad \text{(B3)}$$

$$\mathcal{M}^{(4)}{}_{(j)}\bar{h}^{(j)} = \frac{1}{4}f'[i\omega(\bar{h}^{(5)} - \bar{h}^{(4)}) + \bar{h}^{(4)}_{,r_*} - \bar{h}^{(5)}_{,r_*}] - \frac{1}{2}\ell(\ell+1)\frac{f}{r^2}\bar{h}^{(2)}$$
$$- \frac{ff'}{4r}(3\bar{h}^{(4)} + 2\bar{h}^{(5)} - \bar{h}^{(7)} + \ell(\ell+1)\bar{h}^{(6)}), \quad \text{(B4)}$$

$$\mathcal{M}^{(5)}{}_{(j)}\bar{h}^{(j)} = \frac{f}{r^2}\left[\left(1 - \frac{9M}{2r}\right)\bar{h}^{(5)} - \frac{\ell(\ell+1)}{2}(\bar{h}^{(1)} - f\bar{h}^{(3)}) + \frac{1}{2}\left(1 - \frac{3M}{r}\right)(\ell(\ell+1)\bar{h}^{(6)} - \bar{h}^{(7)})\right], \quad \text{(B5)}$$

$$\mathcal{M}^{(6)}{}_{(j)}\bar{h}^{(j)} = -\frac{f}{2r^2}\left[\bar{h}^{(1)} - \bar{h}^{(5)} - \left(1 - \frac{4M}{r}\right)(\bar{h}^{(3)} + \bar{h}^{(6)})\right], \quad \text{(B6)}$$

$$\mathcal{M}^{(7)}{}_{(j)}\bar{h}^{(j)} = -\frac{f}{2r^2}(\bar{h}^{(7)} + \lambda\bar{h}^{(5)}), \tag{B7}$$

$$\mathcal{M}^{(8)}{}_{(j)}\bar{h}^{(j)} = \frac{1}{4}f'[i\omega(\bar{h}^{(9)} - \bar{h}^{(8)}) + \bar{h}^{(8)}_{,r_*} - \bar{h}^{(9)}_{,r_*}] - \frac{ff'}{4r}(3\bar{h}^{(8)} + 2\bar{h}^{(9)} - \bar{h}^{(10)}), \tag{B8}$$

$$\mathcal{M}^{(9)}{}_{(j)}\bar{h}^{(j)} = \frac{f}{r^2}\left(1 - \frac{9M}{2r}\right)\bar{h}^{(9)} - \frac{f}{2r^2}\left(1 - \frac{3M}{r}\right)\bar{h}^{(10)}, \tag{B9}$$

$$\mathcal{M}^{(10)}{}_{(j)}\bar{h}^{(j)} = -\frac{f}{2r^2}(\bar{h}^{(10)} + \lambda\bar{h}^{(9)}), \tag{B10}$$

where $\lambda = (\ell - 1)(\ell + 2)$.

The sources to the field equation (2.10) take the form

$$\mathcal{J}(r) = -\frac{16\pi E}{f_0^2}\alpha^{(i)}\delta(r - r_0)\begin{cases} Y^{\ell m*}(\pi/2, \Omega_\varphi t), & i = 1, \dots, 7, \\ Y^{\ell m*}_{,\theta}(\pi/2, \Omega_\varphi t), & i = 8, 9, 10, \end{cases} \tag{B11}$$

where

$$\alpha^{(1)} = f_0^2/r_0, \quad \alpha^{(2)} = 0, \quad \alpha^{(3)} = f_0/r_0, \quad \alpha^{(4)} = 2if_0 m\Omega_\varphi, \quad \alpha^{(5)} = 0,$$

$$\alpha^{(6)} = r_0\Omega_\varphi^2, \quad \alpha^{(7)} = r_0\Omega_\varphi^2[\ell(\ell+1) - 2m^2], \quad \alpha^{(8)} = 2f_0\Omega_\varphi, \quad \alpha^{(9)} = 0, \quad \alpha^{(10)} = 2imr_0\Omega_\varphi^2. \tag{B12}$$

APPENDIX C: PUNCTURE FUNCTIONS FOR CIRCULAR ORBITS IN LORENZ GAUGE

In this appendix we give our explicit expressions for the Lorenz-gauge puncture fields $\bar{h}^{(i)P}_{\ell m}$ for the case of a circular geodesic orbit in Schwarzschild spacetime. These punctures contain all pieces of the Detweiler-Whiting singular field necessary to compute the regularized components of the metric and its first derivatives. Written as tensor-harmonic modes in the (θ, φ) coordinate system, the punctures are given by

$$\bar{h}^{(1)P}_{\ell m} = rD^\ell_{m,0}\sqrt{\frac{4\pi}{2\ell+1}}\left[\frac{8(r_0 - 2M)^{3/2}\mathcal{K}}{\pi r_0^2(r_0 - 3M)^{1/2}} - (2\ell + 1)|\Delta r|\frac{2(r_0 - 2M)}{r_0^{5/2}(r_0 - 3M)^{1/2}} + \Delta r\frac{4(r_0 - 2M)^{1/2}[(r_0 - 2M)\mathcal{E} - 2(r_0 - 4M)\mathcal{K}]}{\pi r_0^3(r_0 - 3M)^{1/2}}\right], \tag{C1}$$

$$\bar{h}^{(2)P}_{\ell m} = rf(r)[D^\ell_{m,1} - D^\ell_{m,-1}]\sqrt{\frac{4\pi}{2\ell+1}}\sqrt{\frac{1}{\ell(\ell+1)}}\left[\frac{64(r_0 - 2M)^{1/2}[(r_0 - 2M)\mathcal{E} - (r_0 - 3M)\mathcal{K}]}{\pi r_0^{3/2}M^{1/2}(r_0 - 3M)^{1/2}}\Lambda_1\right], \tag{C2}$$

$$\bar{h}^{(3)P}_{\ell m} = \frac{r}{f(r)}D^\ell_{m,0}\sqrt{\frac{4\pi}{2\ell+1}}\left[\frac{8(r_0 - 2M)^{3/2}\mathcal{K}}{\pi r_0^2(r_0 - 3M)^{1/2}} - (2\ell + 1)|\Delta r|\frac{2(r_0 - 2M)}{r_0^{5/2}(r_0 - 3M)^{1/2}}\right.$$
$$\left. + \Delta r\frac{4(r_0 - 2M)^{1/2}[(r_0 - 2M)\mathcal{E} - 2(r_0 - 4M)\mathcal{K}]}{\pi r_0^3(r_0 - 3M)^{1/2}}\right], \tag{C3}$$

$$\bar{h}^{(4)P}_{\ell m} = \ell(\ell+1)[D^\ell_{m,1} - D^\ell_{m,-1}]\sqrt{\frac{4\pi}{2\ell+1}}\sqrt{\frac{1}{\ell(\ell+1)}}\left[-\frac{64(r_0 - 2M)^{3/2}(\mathcal{E} - \mathcal{K})}{\pi M^{1/2}r_0^{1/2}(r_0 - 3M)^{1/2}}\Lambda_1\right.$$
$$+ \frac{48(r_0 - 2M)^{1/2}[2(r_0 - 2M)\mathcal{E} - (2r_0 - 5M)\mathcal{K}]}{\pi M^{1/2}r_0^{1/2}(r_0 - 3M)^{1/2}(2\ell - 1)(2\ell + 3)} - (2\ell + 1)|\Delta r|\frac{2M^{1/2}}{r_0(r_0 - 3M)^{1/2}}$$
$$+ \Delta r\left(\frac{32(r_0 - 2M)^{1/2}[(r_0 - 4M)\mathcal{E} - (r_0 - 5M)\mathcal{K}]}{\pi M^{1/2}r_0^{3/2}(r_0 - 3M)^{1/2}}\Lambda_1\right.$$
$$\left.\left. - \frac{24[(r_0 - 2M)(2r_0 - 9M)\mathcal{E} - 2(11M^2 - 7Mr_0 + r_0^2)\mathcal{K}]}{\pi M^{1/2}r_0^{3/2}(r_0 - 3M)^{1/2}(r_0 - 2M)^{1/2}(2\ell - 1)(2\ell + 3)}\right)\right], \tag{C4}$$

$$
\bar{h}_{\ell m}^{(5)\mathrm{P}} = \ell(\ell+1)f(r)[D_{m,2}^{\ell} + D_{m,-2}^{\ell}]\sqrt{\frac{4\pi}{2\ell+1}}\sqrt{\frac{1}{(\ell-1)\ell(\ell+1)(\ell+2)}}
$$

$$
\times \left[\frac{256[(4r_0-11M)(r_0-2M)\mathcal{E} - (4r_0-9M)(r_0-3M)\mathcal{K}]}{\pi M(r_0-2M)^{1/2}(r_0-3M)^{1/2}}\Lambda_2 \right.
$$

$$
\left. - \frac{(\ell-1)(\ell+2)}{(2\ell-3)(2\ell-1)(2\ell+3)(2\ell+5)} \frac{640[(8r_0-23M)(r_0-2M)\mathcal{E} - (8r_0-19M)(r_0-3M)\mathcal{K}]}{\pi M(r_0-2M)^{1/2}(r_0-3M)^{1/2}} \right]
$$

$$
+ f(r)D_{m,0}^{\ell}\sqrt{\frac{4\pi}{2\ell+1}}\left[\frac{64[-(r_0-2M)\mathcal{E} + (r_0-3M)\mathcal{K}]}{\pi(r_0-2M)^{1/2}(r_0-3M)^{1/2}}\Lambda_1 \right], \tag{C5}
$$

$$
\bar{h}_{\ell m}^{(6)\mathrm{P}} = \frac{1}{r}D_{m,0}^{\ell}\sqrt{\frac{4\pi}{2\ell+1}}\left[\frac{8Mr_0\mathcal{K}}{\pi(r_0-2M)^{1/2}(r_0-3M)^{1/2}} - (2\ell+1)|\Delta r|\frac{2Mr_0^{1/2}}{(r_0-2M)(r_0-3M)^{1/2}} \right.
$$

$$
\left. + \Delta r\frac{4M(\mathcal{E}+2\mathcal{K})}{\pi(r_0-2M)^{1/2}(r_0-3M)^{1/2}} \right], \tag{C6}
$$

$$
\bar{h}_{\ell m}^{(7)\mathrm{P}} = \frac{(\ell-1)\ell(\ell+1)(\ell+2)}{r}[D_{m,-2}^{\ell} + D_{m,2}^{\ell}]\sqrt{\frac{4\pi}{2\ell+1}}\sqrt{\frac{1}{(\ell-1)\ell(\ell+1)(\ell+2)}}
$$

$$
\times \left[-\frac{128r_0[4(r_0-2M)(2r_0-5M)\mathcal{E} - (8r_0^2-40Mr_0+51M^2)\mathcal{K}]}{3\pi M(r_0-2M)^{1/2}(r_0-3M)^{1/2}}\Lambda_2 \right.
$$

$$
+ \frac{1}{(2\ell-1)(2\ell+3)}\frac{160r_0[8(r_0-2M)(2r_0-5M)\mathcal{E} - (4r_0-9M)(4r_0-11M)\mathcal{K}]}{3\pi M(r_0-2M)^{1/2}(r_0-3M)^{1/2}}
$$

$$
- (2\ell+1)|\Delta r|\frac{Mr_0^{1/2}}{(r_0-2M)(r_0-3M)^{1/2}} + \Delta r\left(\frac{64[(8r_0^2-48Mr_0+67M^2)\mathcal{E} - 2(4r_0^2-26Mr_0+39M^2)\mathcal{K}]}{3\pi M(r_0-2M)^{1/2}(r_0-3M)^{1/2}}\Lambda_2 \right.
$$

$$
\left. \left. - \frac{1}{(2\ell-1)(2\ell+3)}\frac{80[(16r_0^2-96Mr_0+131M^2)\mathcal{E} - 2(8r_0^2-52Mr_0+81M^2)\mathcal{K}]}{3\pi M(r_0-2M)^{1/2}(r_0-3M)^{1/2}} \right) \right], \tag{C7}
$$

$$
\bar{h}_{\ell m}^{(8)\mathrm{P}} = i\ell(\ell+1)[D_{m,1}^{\ell} + D_{m,-1}^{\ell}]\sqrt{\frac{4\pi}{2\ell+1}}\sqrt{\frac{1}{\ell(\ell+1)}}\left[-\frac{64(r_0-2M)^{1/2}((r_0-2M)\mathcal{E} - (r_0-3M)\mathcal{K})}{\pi M^{1/2}r_0^{1/2}(r_0-3M)^{1/2}}\Lambda_1 \right.
$$

$$
+ \frac{1}{(2\ell-1)(2\ell+3)}\frac{48(r_0-2M)^{1/2}[2(r_0-2M)\mathcal{E} - (2r_0-5M)\mathcal{K}]}{\pi M^{1/2}r_0^{1/2}(r_0-3M)^{1/2}} + (2\ell+1)|\Delta r|\frac{2M^{1/2}}{r_0(r_0-3M)^{1/2}}
$$

$$
+ \Delta r\left(\frac{32[(r_0-2M)(r_0-5M)\mathcal{E} - (r_0-3M)(r_0-4M)\mathcal{K}]}{\pi M^{1/2}r_0^{3/2}(r_0-2M)^{1/2}(r_0-3M)^{1/2}}\Lambda_1 \right.
$$

$$
\left. \left. - \frac{1}{(2\ell-1)(2\ell+3)}\frac{24[(r_0-2M)(2r_0-9M)\mathcal{E} - 2(11M^2-7Mr_0+r_0^2)\mathcal{K}]}{\pi M^{1/2}r_0^{3/2}(r_0-3M)^{1/2}(r_0-2M)^{1/2}} \right) \right], \tag{C8}
$$

$$
\bar{h}_{\ell m}^{(9)\mathrm{P}} = i\ell(\ell+1)f(r)[D_{m,2}^{\ell} - D_{m,-2}^{\ell}]\sqrt{\frac{4\pi}{2\ell+1}}\sqrt{\frac{1}{(\ell-1)\ell(\ell+1)(\ell+2)}}
$$

$$
\times \left[\frac{512(r_0-3M)^{1/2}[2(r_0-2M)\mathcal{E} - (2r_0-5M)\mathcal{K}]}{\pi M(r_0-2M)^{1/2}}\Lambda_2 \right.
$$

$$
\left. - \frac{(\ell-1)(\ell+2)}{(2\ell-3)(2\ell-1)(2\ell+3)(2\ell+5)}\frac{640[(8r_0-23M)(r_0-2M)\mathcal{E} - (8r_0-19M)(r_0-3M)\mathcal{K}]}{\pi M(r_0-2M)^{1/2}(r_0-3M)^{1/2}} \right], \tag{C9}
$$

$$\bar{h}_{\ell m}^{(10)P} = \frac{i(\ell-1)\ell(\ell+1)(\ell+2)}{r}[D_{m,-2}^{\ell} - D_{m,2}^{\ell}]\sqrt{\frac{4\pi}{2\ell+1}}\sqrt{\frac{1}{(\ell-1)\ell(\ell+1)(\ell+2)}}$$

$$\times \left[-\frac{512 r_0(r_0-2M)^{1/2}[(2r_0-5M)\mathcal{E} - 2(r_0-3M)\mathcal{K}]}{3\pi M(r_0-3M)^{1/2}}\Lambda_2 \right.$$

$$+ \frac{1}{(2\ell-1)(2\ell+3)}\frac{160 r_0[8(r_0-2M)(2r_0-5M)\mathcal{E} - (4r_0-9M)(4r_0-11M)\mathcal{K}]}{3\pi M(r_0-2M)^{1/2}(r_0-3M)^{1/2}}$$

$$+ (2\ell+1)|\Delta r|\frac{M r_0^{1/2}}{(r_0-2M)(r_0-3M)^{1/2}} + \Delta r\left(\frac{256[2(r_0-4M)(r_0-2M)\mathcal{E} - (r_0-3M)(2r_0-7M)\mathcal{K}]}{3\pi M(r_0-2M)^{1/2}(r_0-3M)^{1/2}}\Lambda_2\right.$$

$$\left.\left. - \frac{1}{(2\ell-1)(2\ell+3)}\frac{80[(16r_0^2-96Mr_0+131M^2)\mathcal{E} - 2(8r_0^2-52Mr_0+81M^2)\mathcal{K}]}{3\pi M(r_0-2M)^{1/2}(r_0-3M)^{1/2}}\right)\right], \tag{C10}$$

where $D_{mm'}^{\ell} \equiv D_{mm'}^{\ell}(\pi, \pi/2, \pi/2)$ is the Wigner-D matrix corresponding to the rotation from (α, β) coordinates to (θ, φ) coordinates and we recall that Λ_1 and Λ_2 are defined in Eqs. (4.9) and (4.10), respectively.

APPENDIX D: MONOPOLE CONTRIBUTION TO THE LORENZ-GAUGE METRIC PERTURBATION

In this section we calculate the monopole ($\ell = 0$) contribution to the retarded and residual metric perturbation at the particle. There is some subtlety to Lorenz-gauge monopole perturbations which we will highlight, but we refer the reader to the given references for more detailed information. We begin by providing the field equations and basis of homogeneous solutions for the monopole perturbation.

1. Field equations and basis of homogeneous solutions

The generic form of the field equations is given by Eq. (2.10). For the monopole perturbation, which has $\ell = 0, m = 0$, and $\omega_m = 0$, only the $(i) = 1, 3, 6$ modes are excited. The field equations can be further simplified using the gauge equation (2.14) to decouple the $\bar{h}^{(6)}$ field; see the discussion around Table I. The remaining field equations for $\bar{h}^{(1)}, \bar{h}^{(3)}$ are given by

$$\bar{h}_{,rr}^{(1)} = -\frac{1}{r^2 f}[(r-4M)\bar{h}_{,r}^{(1)} - \bar{h}^{(1)} - f^2(r\bar{h}_{,r}^{(3)} - \bar{h}^{(3)})], \tag{D1}$$

$$\bar{h}_{,rr}^{(3)} = -\frac{1}{r^2}\left[r\bar{h}_{,r}^{(3)} - \bar{h}^{(3)} + \frac{1}{f^2}((4M-r)\bar{h}_{,r}^{(1)} + \bar{h}^{(1)})\right]. \tag{D2}$$

In order to display the basis of homogeneous solutions, let us define

$$H \equiv (M/\mu)\{h_{tt}, h_{rr}, r^{-2}h_{\theta\theta} = (r\sin\theta)^{-2}h_{\varphi\varphi}\}$$

$$= \frac{M}{4\sqrt{\pi}r}\{\bar{h}^{(1)} + f\bar{h}^{(6)}, f^{-2}(\bar{h}^{(1)} - f\bar{h}^{(6)}), \bar{h}^{(3)}\} \tag{D3}$$

where the second line derives from the metric reconstruction formulas (A43), (A45) and (A48), noting that $Y_{00} = \frac{1}{2\sqrt{\pi}}$. The inverse relations are

$$\bar{h}^{(1)} = 2\sqrt{\pi}\mu^{-1}r(h_{tt} + f^2 h_{rr}), \tag{D4}$$

$$\bar{h}^{(3)} = 4\sqrt{\pi}\mu^{-1}r^{-1}h_{\theta\theta}, \tag{D5}$$

$$\bar{h}^{(6)} = 2\sqrt{\pi}\mu^{-1}\frac{r}{f}(h_{tt} - f^2 h_{rr}). \tag{D6}$$

A complete basis of homogeneous solutions to the two coupled monopole field equations (D1) and (D2) is given by [37]

$$H_A = \{-f, f^{-1}, 1\}, \tag{D7}$$

$$H_B = \left\{-\frac{fM}{r^3}P(r), \frac{f^{-1}}{r^3}Q(r), \frac{f}{r^2}P(r)\right\}, \tag{D8}$$

$$H_C = \left\{-\frac{M^4}{r^4}, \frac{M^3 f^{-2}(3M-2r)}{r^4}, \frac{M^3}{r^3}\right\}, \tag{D9}$$

$$H_D = \left\{\frac{M}{r^4}\left[W(r) + rP(r)f\ln f - 8M^3\ln\frac{r}{M}\right],\right.$$

$$\frac{f^{-2}}{r^4}\left[K(r) - rQ(r)f\ln f - 8M^3(2r-3M)\ln\frac{r}{M}\right],$$

$$\left.\frac{1}{r^3}\left[3r^3 - W(r) - rP(r)f\ln f + 8M^3\ln\frac{r}{M}\right]\right\}, \tag{D10}$$

where

$$P(r) = r^2 + 2rM + 4M^2, \tag{D11}$$

$$Q(r) = r^3 - r^2M - 2rM^2 + 12M^3, \tag{D12}$$

$$W(r) = 3r^3 - r^2M - 4rM^2 - 28M^3/3, \tag{D13}$$

$$K(r) = r^3M - 5r^2M^2 - 20rM^3/3 + 28M^4. \tag{D14}$$

By substitution, it is straightforward to verify that the set $\{H_A, H_B, H_C, H_D\}$ are solutions to the homogeneous field equations (D1) and (D2).

When constructing the inhomogeneous monopole solution it is important to ensure that it represents a particle with the correct mass-energy. That is, by Birkhoff's theorem, for the spherically symmetric monopole perturbation the solution must have the same geometry as the Schwarzschild solution with mass M for $r < r_0$. For $r > r_0$ the solution must again be that of Schwarzschild geometry but with mass $M + \mu E_0$. As we now briefly discuss, perhaps the most natural method for constructing the inhomogeneous monopole perturbation does not satisfy this condition.

First we note that the solutions H_A and H_B are regular at the event horizon but approach nonzero constants as $r \to \infty$. Conversely, H_C and H_D are regular at infinity, but are singular on the horizon. It is therefore tempting to construct the inhomogeneous "internal" solution for $r \le r_0$ as a weighted sum of the $\{H_A, H_B\}$ basis functions and an "external" solution for $r \ge r_0$ as a weighted sum of the $\{H_C, H_D\}$ basis functions. This turns out to not give a solution that has the correct mass-energy [26]. Instead a correction term ΔH_{ih} must be added [37] so that for the retarded field we have

$$H_{\ell=0}^{\text{ret}} = \Delta H_{\text{ih}} + \begin{cases} C_A H_A + C_B H_B, & r \le r_0, \\ C_C H_C + C_D H_D, & r \ge r_0, \end{cases} \quad \text{(D15)}$$

where C_A, C_B, C_C, C_D are constant weighting coefficients and

$$\Delta H_{\text{ih}} = -C_A(H_A - H_B). \quad \text{(D16)}$$

A curious but well understood feature of the Lorenz-gauge monopole perturbation is that the tt component approaches a nonzero constant at infinity [13,40]. When computing gauge-invariant quantities, care must be taken to account for this minor peculiarity of the Lorenz gauge, as discussed in Refs. [26,66,67] (for circular orbits) and Refs. [34,68,69] (for eccentric orbits).

Before we proceed it will be useful to define a matrix of homogeneous solutions by

$$\Phi = \begin{pmatrix} -\bar{h}_A^{(1)} & -\bar{h}_B^{(1)} & \bar{h}_C^{(1)} & \bar{h}_D^{(1)} \\ -\bar{h}_A^{(3)} & -\bar{h}_B^{(3)} & \bar{h}_C^{(3)} & \bar{h}_D^{(3)} \\ -\bar{h}_{A,r}^{(1)} & -\bar{h}_{B,r}^{(1)} & \bar{h}_{C,r}^{(1)} & \bar{h}_{D,r}^{(1)} \\ -\bar{h}_{A,r}^{(3)} & -\bar{h}_{B,r}^{(3)} & \bar{h}_{C,r}^{(3)} & \bar{h}_{D,r}^{(3)} \end{pmatrix}, \quad \text{(D17)}$$

where the matrix elements are constructed by applying the relations (D4) and (D5) to the basis of homogeneous solutions (D7)–(D10).

2. Retarded solution for the monopole mode

The retarded field at the particle is constructed via Eq. (2.21) where the sources are given by

$$\mathcal{J}^{(1)} = -\frac{8E_0\sqrt{\pi}}{r_0}, \qquad \mathcal{J}^{(3)} = \frac{\mathcal{J}^{(1)}}{f_0}. \quad \text{(D18)}$$

Following Eq. (2.22), the (r-independent) coefficients are given by

$$(C_A \ C_B \ C_C \ C_D)^T = \Phi^{-1}.(0 \ 0 \ \mathcal{J}^{(1)} \ \mathcal{J}^{(3)})^T. \quad \text{(D19)}$$

Explicitly, the weighting coefficients take the form

$$C_A = -\frac{2M}{\sqrt{r_0(r_0 - 3M)}}, \quad \text{(D20)}$$

$$C_B = \frac{8M + (6M - 2r_0)\ln f}{3\sqrt{r_0(r_0 - 3M)}}, \quad \text{(D21)}$$

$$C_C = \frac{2[8Mr_0 - 3r_0^2 - 12M^2 + 24M(3M - r_0)\ln\frac{r_0}{M}]}{9M\sqrt{r_0(r_0 - 3M)}}, \quad \text{(D22)}$$

$$C_D = \frac{2}{3}\sqrt{1 - \frac{3M}{r_0}}. \quad \text{(D23)}$$

The monopole contribution to the retarded metric perturbation everywhere in the spacetime is then given by Eq. (D15).

3. Residual solution for the monopole mode

The residual metric perturbation is constructed using Eq. (4.24) and Eq. (4.25). The effective sources $S^{(i)\text{eff}}$ that appear in the latter equation are constructed by making the replacements $\bar{h}^{(1/3)} \to \mathcal{W}\bar{h}^{(1/3)P}$ in Eqs. (D4) and (D5) for $S^{(1)\text{eff}}$ and $S^{(3)\text{eff}}$, respectively. The two necessary punctures are given by Eqs. (C1) and (C3) and $\mathcal{W}$ is the window function. The resulting effective sources are rather cumbersome so we will not display them but they are easily constructed using computer algebra packages.

Following Eq. (4.24), the (r-dependent) weighting coefficients can be solved for via

$$(C_A^{\text{res}} \ C_B^{\text{res}} \ C_C^{\text{res}} \ C_D^{\text{res}})^T = \int_a^b \Phi^{-1}(0 \ 0 \ S^{(1)\text{eff}} \ S^{(3)\text{eff}})^T dr, \quad \text{(D24)}$$

where for C_A and C_B the limits on the integral are $a = r, b = \infty$ and for C_C and C_D the limits are $a = 2M, b = r$. The monopole contribution to the residual metric perturbation everywhere in the spacetime is then given by

$$H_{\ell=0}^{\text{res}}(r) = \Delta H_{\text{ih}} + C_A^{\text{res}}(r)H_A(r) + C_B(r)^{\text{res}}H_B(r) \\ + C_C(r)^{\text{res}}H_C(r) + C_D^{\text{res}}(r)H_D(r). \quad \text{(D25)}$$

Here, although we are calculating the residual field, ΔH_{ih} is still given by Eq. (D16) with constant C_A and C_B calculated via Eq. (D19).

[1] A. H. Mroué, M. A. Scheel, B. Szilágyi, H. P. Pfeiffer, M. Boyle, D. A. Hemberger, L. E. Kidder, G. Lovelace, S. Ossokine, N. W. Taylor, A. Zenginoğlu, L. T. Buchman, T. Chu, E. Foley, M. Giesler, R. Owen, and S. A. Teukolsky, Phys. Rev. Lett. **111**, 241104 (2013).

[2] S. Bernuzzi, A. Nagar, T. Dietrich, and T. Damour, Phys. Rev. Lett. **114**, 161103 (2015).

[3] L. Blanchet, Living Rev. Relativity **17**, 2 (2014).

[4] S. Drasco and S. A. Hughes, Phys. Rev. D **73**, 024027 (2006).

[5] R. Fujita, W. Hikida, and H. Tagoshi, Prog. Theor. Phys. **121**, 843 (2009).

[6] Y. Mino, M. Sasaki, and T. Tanaka, Phys. Rev. D **55**, 3457 (1997).

[7] T. C. Quinn and R. M. Wald, Phys. Rev. D **56**, 3381 (1997).

[8] E. Poisson, A. Pound, and I. Vega, Living Rev. Relativity **14**, 7 (2011).

[9] A. Pound, Phys. Rev. Lett. **109**, 051101 (2012).

[10] S. E. Gralla, Phys. Rev. D **85**, 124011 (2012).

[11] S. Detweiler, Phys. Rev. D **85**, 044048 (2012).

[12] B. Wardell, in Equations of Motion in Relativistic Gravity, edited by D. Puetzfeld, C. Laemmerzahl, and B. F. Schutz (Springer, Berlin, 2015).

[13] S. Detweiler, Phys. Rev. D **77**, 124026 (2008).

[14] S. R. Dolan, N. Warburton, A. I. Harte, A. Le Tiec, B. Wardell, and L. Barack, Phys. Rev. D **89**, 064011 (2014).

[15] S. R. Dolan, P. Nolan, A. C. Ottewill, N. Warburton, and B. Wardell, Phys. Rev. D **91**, 023009 (2015).

[16] P. Nolan, C. Kavanagh, S. R. Dolan, A. C. Ottewill, N. Warburton, and B. Wardell, arXiv:1505.04447 [Phys. Rev. D (to be published)].

[17] A. Le Tiec, A. H. Mroué, L. Barack, A. Buonanno, H. P. Pfeiffer, N. Sago, and A. Taracchini, Phys. Rev. Lett. **107**, 141101 (2011).

[18] S. Akcay, L. Barack, T. Damour, and N. Sago, Phys. Rev. D **86**, 104041 (2012).

[19] D. Bini and T. Damour, Phys. Rev. D **90**, 024039 (2014).

[20] D. Bini and T. Damour, Phys. Rev. D **90**, 124037 (2014).

[21] L. Barack and A. Ori, Phys. Rev. D **61**, 061502 (2000).

[22] L. Barack and D. A. Golbourn, Phys. Rev. D **76**, 044020 (2007).

[23] I. Vega and S. Detweiler, Phys. Rev. D **77**, 084008 (2008).

[24] A. Pound, Phys. Rev. D **90**, 084039 (2014).

[25] A. Pound and J. Miller, Phys. Rev. D **89**, 104020 (2014).

[26] S. R. Dolan and L. Barack, Phys. Rev. D **87**, 084066 (2013).

[27] S. Dolan, Approaches to self-force calculations on Kerr spacetime, in 16th Capra Meeting on Radiation Reaction in General Relativity (to be published), http://maths.ucd.ie/capra16/talks/Dolan.pdf.

[28] N. Warburton and B. Wardell, Phys. Rev. D **89**, 044046 (2014).

[29] S. Hopper, E. Forseth, T. Osburn, and C. R. Evans, Phys. Rev. D **92**, 044048 (2015).

[30] S. A. Teukolsky, Phys. Rev. Lett. **29**, 1114 (1972).

[31] S. A. Teukolsky, Astrophys. J. **185**, 635 (1973).

[32] C. W. Misner, K. Thorne, and J. Wheeler, Gravitation (Freeman, San Francisco, 1973).

[33] L. Barack and N. Sago, Phys. Rev. D **75**, 064021 (2007).

[34] L. Barack and N. Sago, Phys. Rev. D **81**, 084021 (2010).

[35] L. Barack and C. O. Lousto, Phys. Rev. D **72**, 104026 (2005).

[36] S. Akcay, Phys. Rev. D **83**, 124026 (2011).

[37] S. Akcay, N. Warburton, and L. Barack, Phys. Rev. D **88**, 104009 (2013).

[38] T. Osburn, E. Forseth, C. R. Evans, and S. Hopper, Phys. Rev. D **90**, 104031 (2014).

[39] L. Barack and C. O. Lousto, Phys. Rev. D **66**, 061502 (2002).

[40] S. Detweiler and E. Poisson, Phys. Rev. D **69**, 084019 (2004).

[41] S. Detweiler and B. F. Whiting, Phys. Rev. D **67**, 024025 (2003).

[42] L. Barack, Y. Mino, H. Nakano, A. Ori, and M. Sasaki, Phys. Rev. Lett. **88**, 091101 (2002).

[43] L. Barack and A. Ori, Phys. Rev. Lett. **90**, 111101 (2003).

[44] S. Detweiler, E. Messaritaki, and B. F. Whiting, Phys. Rev. D **67**, 104016 (2003).

[45] A. Heffernan, A. Ottewill, and B. Wardell, Phys. Rev. D **86**, 104023 (2012).

[46] N. Warburton, Ph.D. thesis, University of Southampton, 2012.

[47] J. Hadamard, Lectures on Cauchy's Problem in Linear Partial Differential Equations (Dover, New York, 1923).

[48] F. G. Friedlander, The Wave Equation on a Curved Spacetime (Cambridge University Press, Cambridge, England, 1975).

[49] L. Barack and A. Ori, Phys. Rev. D **66**, 084022 (2002).

[50] L. Barack and A. Ori, Phys. Rev. D **67**, 024029 (2003).

[51] R. Haas and E. Poisson, Phys. Rev. D **74**, 044009 (2006).

[52] A. Heffernan, A. Ottewill, and B. Wardell, Phys. Rev. D **89**, 024030 (2014).

[53] I. Vega, P. Diener, W. Tichy, and S. Detweiler, Phys. Rev. D **80**, 084021 (2009).

[54] L. Barack, J. Miller, and A. Pound (private communication).

[55] L. Barack, A. Ori, and N. Sago, Phys. Rev. D **78**, 084021 (2008).

[56] D. A. Golbourn, Ph.D. thesis, University of Southampton, 2009.

[57] See Supplemental Material at http://link.aps.org/supplemental/10.1103/PhysRevD.92.084019 for our high-order punctures which produce a C^2 residual field.

[58] T. Hinderer and É. É. Flanagan, Phys. Rev. D **78**, 064028 (2008).

[59] Wolfram Research, Inc., MATHEMATICA, Version 9.0 (Champaign, Illinois, 2012).

[60] K. S. Thorne, Rev. Mod. Phys. **52**, 299 (1980).

[61] K. Martel and E. Poisson, Phys. Rev. D **71**, 104003 (2005).

[62] R. Haas, arXiv:1112.3707.

[63] E. P. Wigner, Gruppentheorie und ihre Anwendungen auf die Quantenmechanik der Atomspektren (Vieweg Verlag, Braunschweig, 1931).

[64] M. E. Rose, Elementary Theory of Angular Momentum (Wiley, New York, 1957).

[65] A. Challinor, P. Fosalba, D. Mortlock, M. Ashdown, B. Wandelt, and K. Górski, Phys. Rev. D **62**, 123002 (2000).

[66] N. Sago, L. Barack, and S. Detweiler, Phys. Rev. D **78**, 124024 (2008).

[67] T. Damour, Phys. Rev. D **81**, 024017 (2010).

[68] L. Barack and N. Sago, Phys. Rev. D **83**, 084023 (2011).

[69] S. Akcay, A. Le Tiec, L. Barack, N. Sago, and N. Warburton, Phys. Rev. D **91**, 124014 (2015).